研究成果の刊行に関する一覧表

発表者氏名	論文タイトル名	発表誌名	巻号	ページ	出版年
Ozaki T, Anas C, Maruyama S, Yamamoto T, Yasuda K, Morita Y, Ito Y, Gotoh M, Yuzawa Y, Matsuo S	Intrarenal administration of recombinant human soluble thrombomodulin ameliorates ischaemic acute renal failure	Nephrol Dial Transplant	23(1)	110-119	2007
Anas C, Ozaki T, Maruyama S, Yamamoto T, Gotoh M, Ono Y, Matsuo S	Effects of Olprinone, a phosphodiesterase III inhibitor, on ischemic acute renal failure	Int J Urol	14(3)	219-225	2007
Kinomura M, Kitamura S, Tanabe K, Ichinose K, Hirokoshi K, Takazawa Y, Kitayama H, Nasu T, Sugiyama H, Yamasaki Y, Sugaya T, Maeshima Y , Makino H	Amelioration of cisplatin-induced acute renal injury by renal progenitor-like cells derived from the adult rat kidney	Cell trans-plantation	(in press)		2008
Negishi K, Noiri E, Maeda R, Portilla D, Sugaya T, Fujita T	Renal L-type fatty acid-binding protein mediates the bezafibrate reductionof cisplatin-induced acute kidney injury	Kidney Int	(in press)		2008

雑誌

発表者氏名	論文タイトル名	発表誌名	巻号	ページ	出版年
山本徳則，菅谷健，野入英世，山田伸，上平修，絹川常郎，小松智徳，松川宣久，吉野能，服部良平，大島伸一，後藤百万	新しい腎虚血バイオマーカ：RenalLtype-FABP(L-FABP)	日本腎予防医学研究会雑誌	掲載予定		2008

Renal L-Type Fatty Acid–Binding Protein in Acute Ischemic Injury

Tokunori Yamamoto,* Eisei Noiri,† Yoshinari Ono,* Kent Doi,† Kousuke Negishi,† Atsuko Kamijo,‡ Kenjiro Kimura,‡ Toshiro Fujita,† Tsuneo Kinukawa,§ Hideki Taniguchi,‖ Kazuo Nakamura,¶ Momokazu Goto,* Naoshi Shinozaki,** Shinichi Ohshima,†† and Takeshi Sugaya‖**

*Department of Urology, University Hospital, Nagoya University, Nagoya, †Departments of Nephrology and Endocrinology, Hemodialysis and Apheresis, University Hospital, and Center of NanoBio Integration, University of Tokyo, Tokyo, ‡Department of Nephrology and Hypertension, St. Marianna University, Kawasaki, §Department of Urology, Chukyo Hospital, Nagoya, ‖Center for Developmental Biology, Riken, Kobe, ¶CMIC Co., Ltd., Tokyo, **Cornea Center, Tokyo Dental College Ichikawa General Hospital, Tokyo, and ††National Center for Geriatrics and Gerontology, Obu, Japan

ABSTRACT

Fatty acid–binding proteins (FABPs) bind unsaturated fatty acids and lipid peroxidation products during tissue injury from hypoxia. We evaluated the potential role of L-type FABP (L-FABP) as a biomarker of renal ischemia in both human kidney transplant patients and animal models. Urinary L-FABP levels were measured in the first urine produced from 12 living-related kidney transplant patients immediately after reperfusion of their transplanted organs, and intravital video analysis of peritubular capillary blood flow was performed simultaneously. A significant direct correlation was found between urinary L-FABP level and both peritubular capillary blood flow and the ischemic time of the transplanted kidney (both $P < 0.0001$), as well as hospital stay ($P < 0.05$). In human-L-FABP transgenic mice subjected to ischemia-reperfusion injury, immunohistological analyses demonstrated the transition of L-FABP from the cytoplasm of proximal tubular cells to the tubular lumen. In addition, after injury, these transgenic mice demonstrated lower blood urea nitrogen levels and less histological injury than injured wild-type mice, likely due to a reduction of tissue hypoxia. *In vitro* experiments using a stable cell line of mouse proximal tubule cells transfected with h-L-FABP cDNA showed reduction of oxidative stress during hypoxia compared to untransfected cells. Taken together, these data show that increased urinary L-FABP after ischemic-reperfusion injury may find future use as a biomarker of acute ischemic injury.

J Am Soc Nephrol 18: 2894–2902, 2007. doi: 10.1681/ASN.2007010097

Mammalian intracellular fatty acid–binding proteins (FABP) are expressed from a large multigene family and encode 14-kD proteins that are members of the superfamily of lipid-binding proteins (LBP).[1] There are nine different FABP with tissue-specific distribution that include liver, intestinal, muscle and heart, adipocyte, epidermal, ileal, brain, myelin, and testis.[2] The epithelial FABP is unique among the LBP because of the presence of six cysteine residues, two of which, Cys-120 and -127, are modeled to form a disulfide bond within the ligand binding cavity. One report[3] showed that 4-hydroxynonenal (HNE), a cytotoxic α,β-unsaturated acyl aldehyde produced from lipid peroxidation in response to oxidative stress, was able to modify the Cys-120 residue of E-FABP. Similarly, Wang *et al.*[4]

Received January 23, 2007. Accepted June 14, 2007.

Published online ahead of print. Publication date available at www.jasn.org.

Correspondence: Dr. Eisei Noiri, 107 Lab, Nephrology, University Hospital, University of Tokyo, 7-3-1 Hongo, Bunkyo, Tokyo, Japan 113-8655. Phone/Fax: 81-3-5814-8696; E-mail: noiri-1im@h.u-tokyo.ac.jp

demonstrated *in vitro* the potentiality of L-type FABP (L-FABP) to reduce oxidative stress in hypoxia-reoxygenation. When they increased the level of L-FABP expression, the intracellular oxidative stress was less. These studies, together with other studies,[5–7] have shown that FABP not only participate in fatty acid trafficking but also serve as early indicators of ischemic conditions and as important protective cellular antioxidant molecules that inactivate reactive lipids.

In the human kidney, L-FABP is expressed predominantly in the proximal tubules, a nephron segment that uses fatty acids as the major source of energy metabolism.[8] The role that L-FABP plays in ischemic injury has not been previously examined. Recent refinement of the previously described intravital video microscopy,[9] combined with sophisticated image analysis, has allowed us to monitor microcirculation in humans in a minimally invasive manner. In this study, we examined the role of L-FABP in ischemic conditions using the human model of kidney transplantation. This model is one of the most suitable models to evaluate a potential relationship between capillary blood flow and urinary parameters of acute kidney injury. Our results provide direct evidence that increased urinary levels of human L-FABP could represent an early biomarker of human renal ischemia. Furthermore, in concurrent studies using human L-FABP transgenic (h-L-FABP-Tg) mice, our results suggest that the expression of renal L-FABP protects kidney tissue from renal ischemic stress.

RESULTS

Because the time point of clamping organ blood flow is definite in living-related human renal transplantation, it can be used to monitor a wide variety of pericapillary blood flow. Thus, living-related human renal transplantation provides an especially suitable model for examining the hemodynamics of peritubular capillary blood flow and urinary L-FABP. The actual ischemic time is determined easily and is monitored in each case. Twelve patients who had received living-related kidney transplantation were enrolled for capillary blood flow measurement. Intravital video charge-coupled device (CCD) images revealed a remarkable decrease of peritubular blood flow when measured close to the initiation of reperfusion. That flow gradually increased when measured at times further from reperfusion. The correlations between peritubular blood flow and the urinary markers defined already were examined and are shown in Figure 1. Among those markers, only urinary L-FABP correlated well to the increase of the reciprocal unit of peritubular capillary blood flow (1/blood flow; $n = 12$; $r = 0.933$, $P < 0.0001$); others did not reflect it. Urinary L-FABP becomes detectable when peritubular blood flow slows to <1 mm/s; consequently, the slower the peritubular blood flow, the higher the urinary L-FABP level.

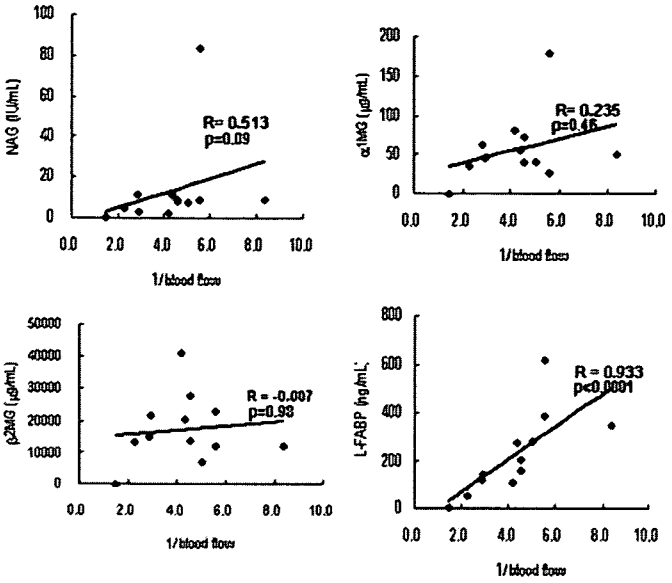

Figure 1. Correlation between peritubular capillary blood flow and urinary markers. Urinary markers are compared with 1/blood flow: Where renal ischemia is more severe, 1/blood flow is larger. Among the urinary markers examined, urinary L-FABP was most closely correlated with the decrease of peritubular blood flow.

We defined the ischemic time as the period between the time point of clamping the donor's renal artery and the time point of the appearance of virgin urine from the recipient's ureter. The urinary L-FABP values of that time point were collected, measured, and plotted together with ischemic time. As shown in Figure 2, urinary L-FABP and ischemic time showed an extremely significant correlation at the level of $r = 0.939$ ($n = 10$; $P < 0.0001$). All transplanted kidneys received renal biopsy 1 h after reperfusion—the so-called 1-h biopsy. Portions of 1-h biopsy specimens were examined immunohistochemically for L-FABP and compared with normal kidney. A representative image is shown in Figure 3. L-FABP was stained predominantly in the cytoplasmic region of normal human proximal tubules, as shown in the Figure 3, top (Normal). It is noteworthy that in ischemic kidney, the localization of L-FABP moved from the proximal tubular cells to the tubular lumen in

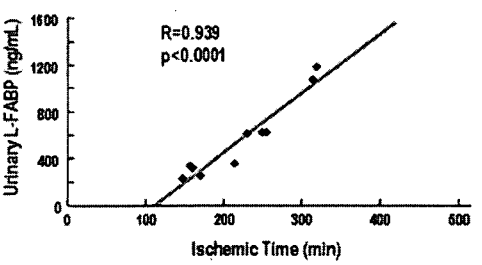

Figure 2. Correlation between ischemic time and urinary L-FABP. The ischemic time in living-related renal transplantation was defined as the period between the time point of clamping the donor's renal artery and the time point of appearance of virgin urine from the recipient's ureter. They showed an extremely significant correlation at the level of $r = 0.939$ ($n = 10$; $P < 0.0001$).

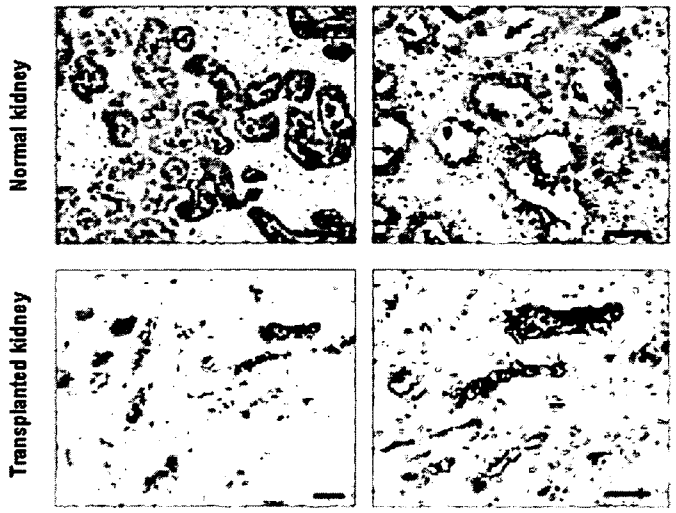

Figure 3. Immunohistochemical distribution of L-FABP. L-FABP was stained predominantly in the cytoplasmic region of the proximal tubule in intact human kidney (Normal kidney). It is noteworthy that the localization of L-FABP moved from the proximal tubular cells to the tubular lumen in a 1-h biopsy obtained from a patient with a successful medical record (Transplanted kidney), where the ischemic time was 4 h. The definition of ischemic time in this study was the period between the time point of clamping the donor's renal artery and the time point of appearance of virgin urine from the recipient's ureter. Bar = 50 μm. Magnifications: ×200 on left; ×400 on right.

a 1-h biopsy obtained from a patient who had a successful urine outcome 1 h after anastomosis in the transplant medical record (Figure 3, right). Because the postoperative renal function is virtually excellent in living-related renal transplantation, the improvement of renal function is very rapid. We observed that the pre- and postoperative levels of blood urea nitrogen (BUN) and serum creatinine (SCr) did not change significantly during the follow-up period. Urine N-acetyl-β-D-glucosaminidase (NAG) and β2-microglobulin levels also did not change during the follow-up period. No patient required renal replacement therapy after transplantation. The only finding obtained from those evaluations was the significant correlation between the hospital stay and urine L-FABP or renal microcirculation, where the correlation of the hospital stay with the initial urine L-FABP level of transplanted kidney was $r = 0.74$ ($n = 12$; $P < 0.05$). The correlation with renal microcirculation was $r = 0.89$ ($n = 12$; $P < 0.05$).

For further confirmation that urinary L-FABP is a biomarker reflecting proximal tubular ischemia, the human L-FABP gene with a 5′ promoter region was transferred to C57Bl/6 mice to obtain h-L-FABP-Tg mice. In these transgenic mice, it was confirmed that L-FABP was expressed predominantly in the proximal tubules, which was comparable to human kidney (Figure 3, Normal).

We next performed 30-min renal ischemia/reperfusion (I/R) injury in both h-L-FABP-Tg and wild-type mice. Blood was drawn sequentially from each mouse until 3 d after ischemia. Figure 4A shows the BUN profiles. The increase of BUN found 15 h after clamp release in the wild-type ischemic mice (110.1 ± 23.7 mg/dl [mean ± SD]; $n = 10$) was ameliorated in the ischemic h-L-FABP-Tg mice (75.0 ± 27.5; $n = 10$). Similarly, SCr increased from 0.22 ± 0.05 to 1.42 ± 0.2 mg/dl ($n = 10$) 15 h after I/R in the wild-type mice (Figure 4B). This increase was significantly ameliorated to a significant level in the ischemic h-L-FABP-Tg mice (1.12 ± 0.15 mg/dl; $n = 10$). The decrease in the ischemic h-L-FABP-Tg group continued at least 72 h after initiation of I/R. Histologic analyses were performed next. The representative histologic images of ischemic kidney 15 h after initiation of I/R are shown in Figure 5. An established protocol for quantification of histologic findings exists in renal I/R[10,11]; therefore, we followed this procedure of scoring for the evaluation, as reported previously.[12,13] Ischemic kidneys obtained from wild-type mice showed remarkable brush border loss, tubular dilation, tubular epithelial cell exfoliation, and widening of peritubular spaces. These findings

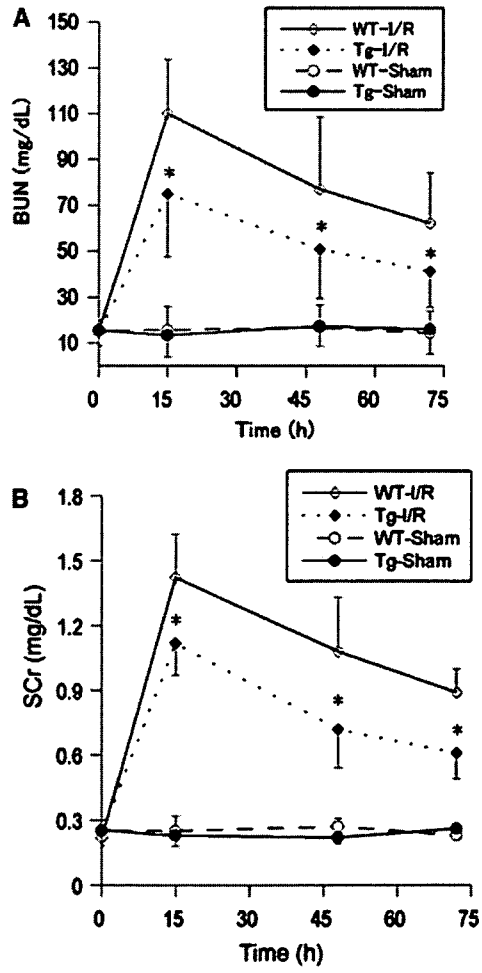

Figure 4. (A) Time course of BUN after renal I/R injury. (B) Time course of SCr after renal I/R injury. h-L-FABP-Tg I/R mice (Tg-I/R) showed half the level of BUN and SCr compared with that of wild-type (WT) I/R mice (WT-I/R) during all courses of experiments. This increase of BUN and SCr was ameliorated significantly in Tg-I/R ($n = 10$; $^*P < 0.05$).

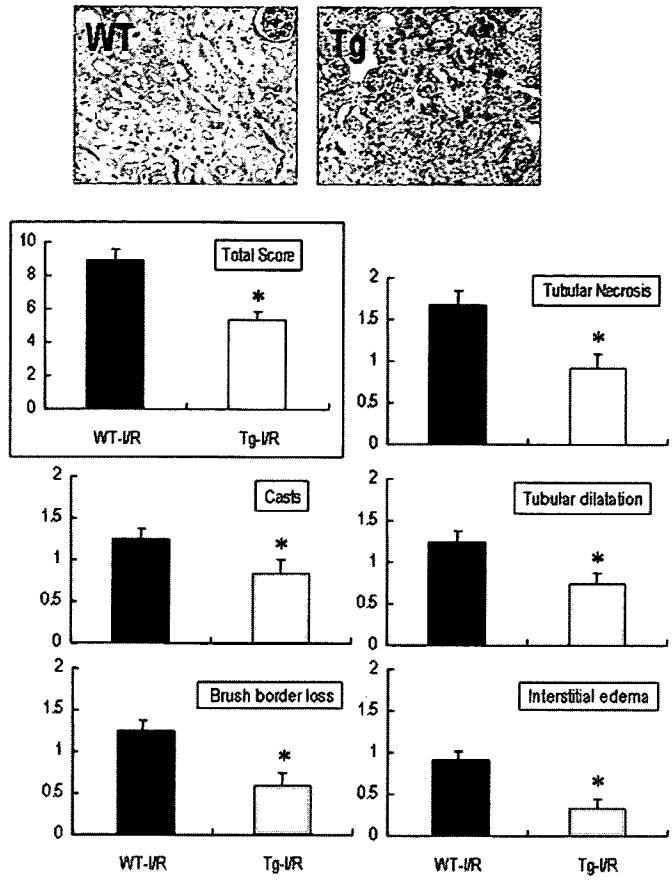

Figure 5. Representative histologies and acute tubular necrosis (ATN) score. Ischemic kidneys obtained from WT mice 15 h after initiation of I/R showed brush border loss, tubular dilation, tubular epithelial cell exfoliation, and widening of the peritubular space. These findings were markedly reduced in h-L-FABP-Tg mice. Each index and total score of those alleviated are shown quantitatively in bar graphs following the established protocol ($n = 10$; $*P < 0.01$).

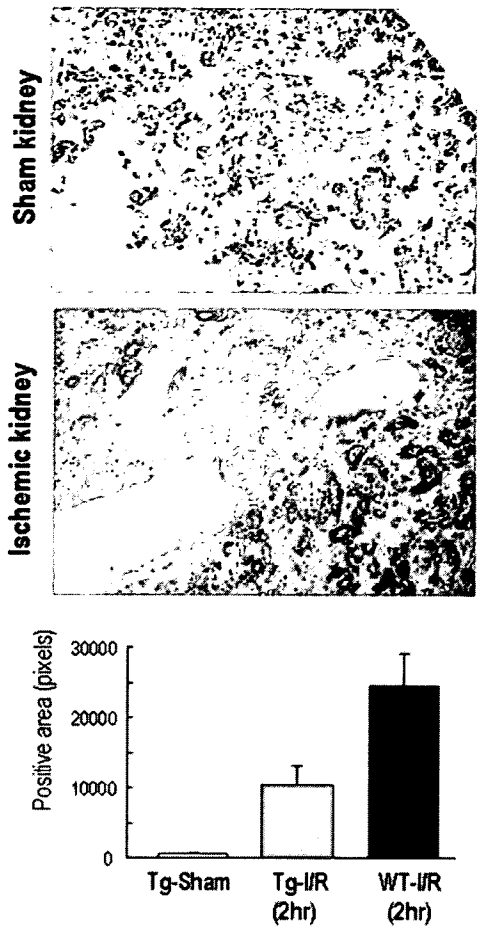

Figure 6. Renal distribution of L-FABP and hypoxia was examined in h-L-FABP-Tg mice subjected to renal I/R. The pimonidazole-positive hypoxic area (brown) expanded significantly in the outer medulla to the cortical region of ischemic h-L-FABP-Tg kidney. This area overlapped hardly at all with that of the L-FABP–positive proximal tubular cells (light green). The pimonidazole-positive hypoxic area was examined quantitatively using an image analysis platform, as summarized in the bar graph.

were significantly reduced in h-L-FABP-Tg kidneys, as shown in the bar graph of Figure 5. A statistically significant reduction was also found in the total scoring of all parameters in h-L-FABP-Tg kidneys.

Recently, it has become possible to demonstrate the hypoxic tissue condition using the hypoxic indicator pimonidazole that creates adducts during 1 to 2 h under oxygen tension of <10 mmHg. The specific antibody raised against this adduct is also commercially available. This system was applied to ischemic h-L-FABP-Tg mice to evaluate the localization of hypoxia and L-FABP. Figure 6, top, demonstrates the localization of both pimonidazole and L-FABP in sham-operated h-L-FABP-Tg kidneys. The L-FABP was clearly apparent in the proximal tubules in the outer medulla to the cortex, and staining of pimonidazole was not found in this group. In ischemic h-L-FABP-Tg kidney obtained 2 h after reperfusion, both pimonidazole and L-FABP were found in the proximal tubules of the outer medulla to the cortex (Figure 6, middle); however, those signals were not mutually overlapping. Hypoxic tubules did not express L-FABP any more at this time point, and/or tubules expressing L-FABP were not sufficiently hypoxic to the level to induce pimonidazole adduct formation. This observation suggests the potentiality that L-FABP is a molecule that preserves proximal tubules under hypoxia and that proximal tubules expressing L-FABP are presumably equivalent to vital tubules even in the ischemic renal condition.

The pimonidazole-positive area of ischemic kidney obtained 2 h after reperfusion was quantified using AIS (Fuji Photo Film, Tokyo, Japan). The pimonidazole-positive hypoxic area was expanded significantly in the outer medulla to the cortical region of ischemic h-L-FABP-Tg kidney compared with the sham-operated h-L-FABP-Tg kidney, whereas the hypoxic area seen in ischemic h-L-FABP-Tg kidney was considerably smaller than that of the ischemic wild-type kidney. Quantitative real-time PCR analyses were performed for kidneys harvested 8 and 24 h after I/R, and urinary L-FABP was

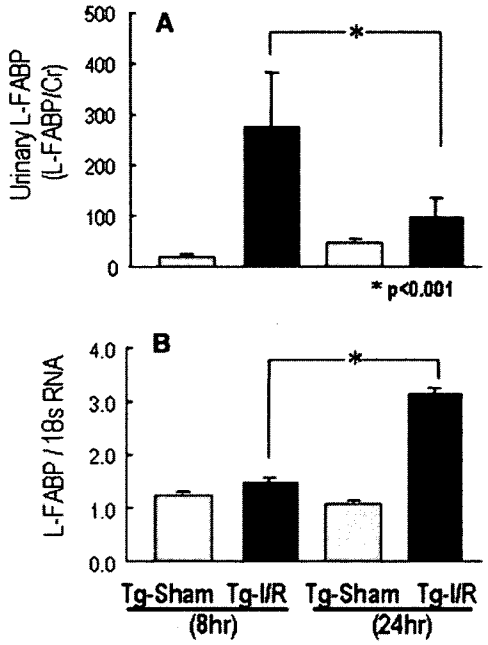

Figure 7. (A) Urinary L-FABP-to-Cr level in ischemic h-L-FABP-Tg mice. (B) Renal L-FABP transcriptional level in ischemic h-L-FABP-Tg mice. Both urine and renal tissue were obtained from the same mouse. A lag existed between urinary excretion of L-FABP and its renal transcription during I/R in h-L-FABP-Tg mice.

simultaneously monitored in the same mice. These combined results are shown in Figure 7. The transcription level of renal L-FABP increased significantly 24 h after reperfusion; that increase was not observed 8 h after I/R. Conversely, the urinary L-FABP level had increased by 8 h after reperfusion; this increase was alleviated 24 h after I/R. The effect of L-FABP on the hypoxic condition was examined *in vitro* with the comparison between mProx and mProx-L. The level of reactive oxygen species (ROS) was measured by CM-H_2DCFDA as previously reported,[13] and it was found that the level was remarkably reduced in mProx-L compared with mProx under hypoxia (Figure 8A, **). The transcription level in mProx-L cells was upregulated to the significant level under hypoxia (Figure 8B). In addition, the h-L-FABP level in the medium was significantly increased in that of hypoxic mProx-L compared with normoxia (Figure 8C).

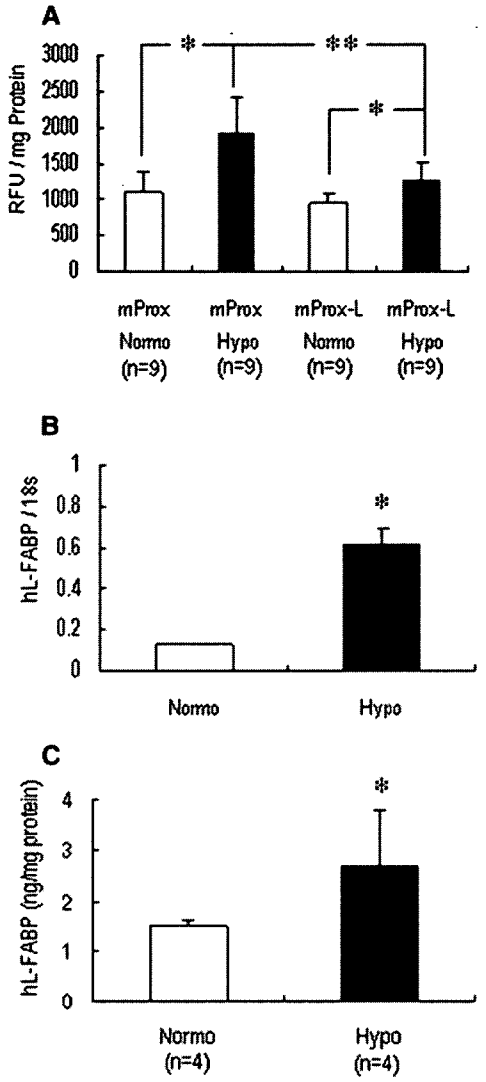

Figure 8. (A) Oxidative stress induced by hypoxia found in mProx was reduced in mProx-L to a significant level. Normo, normoxia; Hypo, hypoxia. The relative fluorescence unit (RFU) was normalized by the protein level. *$P < 0.01$. (B) The transcription level of human L-FABP was upregulated under hypoxia in mProx-L. Note that L-FABP was not expressed in mProx originally obtained from C57Bl/6 mice. Experiments were in quadruplicate. *$P < 0.05$, normoxia *versus* hypoxia; **$P < 0.05$ mProx *versus* mProx-L under hypoxia. (C) The protein level in cultured medium was compared between normoxia and hypoxia. Experiments were in quadruplicate. *$P < 0.05$.

DISCUSSION

The FABP family comprises nine subtypes with organ-specific expression, some of which is linked closely to ischemic tissue conditions. Indeed, the I type of FABP, expressed in the small intestine, has been reported to increase in blood during the acute phase of intestinal artery thrombosis, a clinical condition that is difficult to diagnose in view of contemporary practical skill.[5] It is therefore expected to be the specific diagnostic marker of this disease. Moreover, in patients with acute myocardial infarction, it has been observed that the H type of FABP released from damaged or ischemic cardiac muscle appears in blood at the acute phase.[14] Recently, in comparison with the creatinine kinase MB-isoform or troponin-T, the blood concentration of H-type FABP was most sharply increased in patients visiting emergency departments for chest pain. Sandwich ELISA was found to be particularly useful for discovery of acute coronary syndrome within 6 h after its onset.[6]

In human kidney, L-FABP is expressed predominantly in proximal epithelial tubules, where FABP serves as a target of the highly cytotoxic aldehydes that are inevitably generated from lipid

peroxidation reaction during reperfusion; admittedly, FABP demonstrated its capability to bind with HNE, as demonstrated by Bennaars-Eiden *et al.*[3] The L-FABP presumably traps and transfers HNE to urinary spaces and sheds it into urine. Our study is the first to clarify the direct evidence of L-FABP localization in human proximal tubules with pericapillary blood flow. The translocation of L-FABP to urinary space under the ischemic condition was detectable by the ELISA method.

Given that L-FABP could act as a surrogate molecule that reduces lipid peroxidative stress in proximal tubular cells, the expression and upregulation of L-FABP *per se* might decrease renal ischemic insults. To answer that question, we produced h-L-FABP-Tg mice and subjected them to renal I/R. Tissue hypoxia after I/R was ameliorated remarkably in the presence of L-FABP, thereby demonstrating the orchestration among histologic hypoxia, L-FABP expression, and urinary L-FABP excretion. Admittedly, the reduction of oxidative stress under hypoxia was also more prominent in cells expressing human L-FABP *in vitro*. The upregulation of transcription level and increase of protein level were also confirmed *in vitro*. In addition, the chronological dynamics of the urinary L-FABP and cortical RNA level in h-L-FABP-Tg mice suggested a substantial feedback mechanism related to the promoter region of L-FABP controlling the renal proximal tubular L-FABP level.

It is noteworthy that L-FABP is not expressed in rodent kidney because nucleotides −4000 to −597, which are upstream of the rodents' L-FABP gene in their kidney, contain an orientation-independent suppressor sequence that prohibits renal expression.[15] In other words, rats and mice of wild type are equivalent to renal L-FABP–deficient animals, but renal expression of this molecule is secured in h-L-FABP-Tg mice; therefore, it is conceivable that the humanized kidneys are adopted in h-L-FABP-Tg mice in terms of this molecule. This might explain the discrepancy between findings in humans and rodents and the consequent criticism that the rodent model of acute renal failure, including the I/R model, does not correlate well with that in humans. That critique is related to the failure in clinical trials for acute renal failure that had been anticipated in light of favorable data of animal experiments.[16,17]

Using living-related renal transplantation, we observed the efficacy of urinary L-FABP as a biomarker of peritubular ischemia occurring after renal transplantation, and further found that the initial urine L-FABP level of transplanted kidney was the biomarker directly reflecting clinical outcome in terms of hospital stay. When the urine L-FABP level increased beyond 200 ng/ml, the duration of hospital stay became longer.

This finding was also confirmed in a murine renal I/R model using h-L-FABP-Tg mice. Further investigation is needed to evaluate the efficacy in cadaveric renal transplantation, vascular surgery that stops or reduces renal blood flow, catheter-related intervention that often accompanies renal arterial thromboembolization, and so forth. Urinary L-FABP is also promising for monitoring chronic ischemia, an essential mechanism for progressive chronic kidney disease (CKD). Kamijo *et al.*[18] investigated the urinary level in progressive CKD using a sandwich ELISA method for L-FABP. Their study concluded that the urinary level of L-FABP was the most sensitive indicator able to substantiate the prognosis of renal disease: Its use is superior to that of the SCr level, urinary protein level, or the urinary α1-microglobulin level.[18] Other studies[19,20] emphasized chronic hypoxia in the tubulointerstitium as an alternative unifying mechanism of CKD progression. Chronic hypoxia in the kidney can occur according to structural changes that impair blood flow delivery to the tubules. In the event of glomerular sclerosis and/or interstitial fibrosis, the lesion is occupied by excessive extracellular matrix, which engenders the loss of microvasculature and renders both the lesion and its surrounding area hypoxic. That factor of chronic peritubular ischemia should also be considered as a mechanism of urinary L-FABP excretion in CKD. Furthermore, urinary L-FABP is now anticipated as a biomarker for type 2 diabetic nephropathy.[21]

On the basis of these data, the current hypothesis of L-FABP in renal proximal tubular epithelial cells is shown in Figure 9.

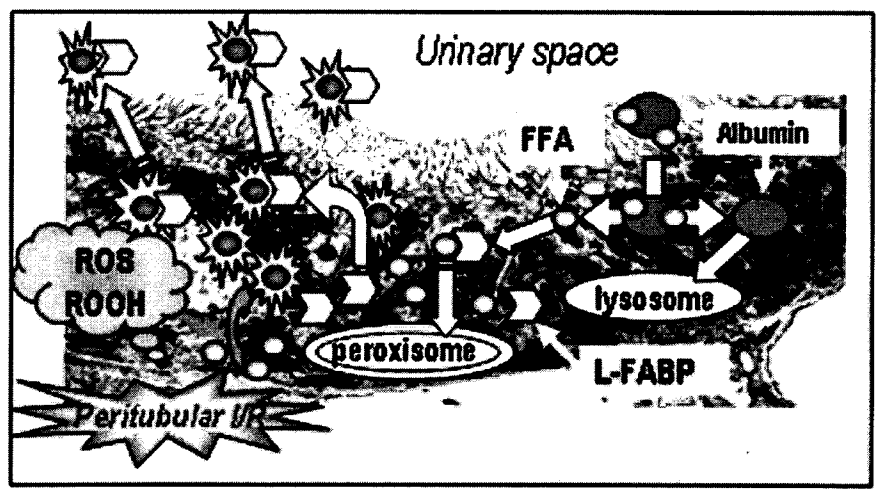

Figure 9. Conceptual schema for the renal L-FABP mechanism. In the kidney, albumin filtered from glomeruli is reabsorbed predominantly in proximal tubules together with free fatty acids (FFA) under physiologic conditions. After reabsorption, cytosolic albumin transfer to lysosome and fatty acid was released and received by L-FABP during this process. Fatty acid–bound L-FABP will usually be relocated to cytosolic peroxisome for size reduction of fatty acids. Under ischemic conditions, lipid peroxidation products will accumulate in proximal tubules and damage proximal tubules (left). L-FABP is presumably capable of binding these noxious lipid peroxidative products and transferring them to urinary spaces. L-FABP is excreted from the proximal tubules into urine by binding cytotoxic lipids. ROOH, hydroperoxide radicals.

Proximal tubular epithelial cells reabsorb >95% of urinary albumin that is filtered through a glomerular slit membrane. Free fatty acid bound to albumin is also incorporated into cellular cytoplasms together with albumin and is used for the β-oxidation–dependent tubular energy metabolic system. The L-FABP in proximal tubular epithelial cells serves as a shuttle of free fatty acid to appropriate cytosolic organella such as peroxisome, mitochondria, and/or extracellular urinary space (presumably a very small amount). In ischemic circumstances in human kidney, unsaturated fatty acids, the chemical characteristics of which are similar to that of detergents, are generated readily from cell membranes and cytoplasmic membranes. They are the major source of lipid-based peroxyradicals and aldehydes that are increased during I/R injury[13,22,23] and therefore propagate cellular injury *via* lipid peroxidation processes. The L-FABP molecule is capable of interrupting this reaction, especially binding fatty acids and aldehydes such as HNE into that pocket of β-sheet structure and relocating their distribution toward the tubular lumen, thereby preventing proximal tubular injury during ischemia and reperfusion.

Human L-FABP-Tg mice endowed with humanized kidneys, in contrast to those of wild-type rodents, are presumably more appropriate for the investigation of a renal disease model targeting human kidney disease. Especially in screening of newly discovered compounds for potential drugs, the h-L-FABP-Tg mouse model is better suited for nephrotoxicologic screening before going to clinical studies; therefore, it is more economical for future drug discovery processes. The characteristics of human L-FABP described here will fit the first and second topics of the Critical Path Opportunity List announced by the US Food and Drug Administration in 2006.

CONCISE METHODS

Protocol to Measure Peritubular Blood Flow and Urinary Markers of Proximal Tubule Injury in Living-Related Kidney Transplant Patients

During 12 living-related kidney transplant operations, peritubular capillary images were obtained using an intravital video CCD. The entire protocol of this study was explained to all patients, and their informed consent was obtained before initiation of the study, according to a protocol approved by the Human Study Committee of Nagoya University. Living-related kidney transplantation was performed using a method we reported previously.[24,25] Renal capillary blood flow was visualized and measured following the previously reported method with the adjustment for human renal capillary flow, as detailed in an online resource.[26] Urinary markers such as NAG, β2-microglobulin, and α1-microglobulin were monitored together with urinary L-FABP for comparison with peritubular capillary blood flow. Those markers except L-FABP were measured by the hospital's clinical pathology department. Urine collection was performed 24 h before transplantation from donors and subsequently performed after reperfusion of the transplanted kidney, where virgin urine and urine of indicated reperfusion time points were separately collected. Initiation of reperfusion is the time point that established anastomosis of the renal artery and vein of the transplanted kidney. Before anastomosis of the ureter, urine was collected directly from the ureter of the transplanted kidney.

h-L-FABP-Tg Mice and the Renal I/R Model

The engineering of h-L-FABP-Tg mice is detailed elsewhere.[27] Briefly, genomic DNA of human L-FABP, including its promoter region (13 kb), was microinjected into fertilized eggs obtained from C57Bl/6 and CBA mice; ICR mice were used as transfected-egg recipients. The resultant transgenic mice were backcrossed for more than nine generations onto C57Bl/6 mice to obtain homozygous mutant mice with an inbred background. Only heterozygous h-L-FABP-Tg mice were used in this experiment. Male wild-type and h-L-FABP-Tg mice weighing 20 to 25 g were allowed food and water *ad libitum*. The mice were anesthetized using a combination of ketamine hydrochloride 11.6 mg/100 g and xylazine hydrochloride 0.77 mg/100 g and placed on a heated surgical pad. Rectal temperature was monitored using a sensitive thermistor for neonates (P1619; Nikkiso-YSI, Tokyo, Japan) with a data logger (600-1075; Barnant, Barrington, IL) and maintained 2°C above the initial core temperature. A 1.5-cm posterior lateral line incision was made, and both kidneys were exposed. Renal ischemia was initiated by clamping both renal arteries using microclips (Fine Science Tools, Foster City, CA). After 30 min, both clamps were removed; renal arteries were subsequently released. The incision was closed using a 3-0 suture and surgical staples. Mice were kept in glass-shielded metabolic cages (Metabolica; Sugiyamagen, Tokyo, Japan) until being killed, and urine was collected. Blood was drawn serially from each tail vein for BUN analyses 15, 48, and 72 h after surgery. Kidney specimens were collected 72 h after clamp release for immunohistochemistry and 2 h after injection of hypoxic probe. In a separate procedure, kidney specimens were collected 8 and 24 h for reverse transcriptase–PCR. All experiments were conducted in accordance with the National Institutes of Health Guide for the Care and Use of Laboratory Animals.

Measurement of BUN and SCr

BUN and SCr were measured following the previously reported method.[28]

Measurement of Urinary h-L-FABP by ELISA

Urinary h-L-FABP was measured by the sandwich ELISA kit following the manufacturer's protocol (CMIC, Tokyo, Japan). When intra-assay reproducibility was determined by the same sample eight times, the coefficient of variation for the obtained value was within 10%. The measurable range of this kit is between 4 and 400 ng/ml. The measurement was performed in duplication. The L-FABP value of healthy individuals including donor urine (before transplantation) was within the range of 0.12 to 20.09 ng/ml, and that mean is 1.60 ng/ml. In a part of the experiment, L-FABP was measured in cell culture medium. This assay system does not detect rodents' L-FABP, particularly that derived from wild type.

Morphologic Evaluation of Kidneys

Formalin-fixed sections were stained with hematoxylin-eosin and periodic acid-Schiff. The morphologic evaluation of I/R injury was performed using well-established criteria in a blind manner.[10–13]

Immunohistochemical Analyses

Immunohistochemical staining of 2-μm paraffin sections was performed using an indirect immunohistochemical technique. After deparaffinization, nonspecific reaction for horseradish peroxidase was blocked by 3% hydrogen peroxide in methyl alcohol for 10 min. Human specimens were subsequently blocked by goat serum (Dako-Japan, Kyoto, Japan). Mice specimens were blocked initially by Blocking A solution of Histofine Mice Stain Kit (Nichirei, Tokyo, Japan) for mouse tissue immunohistochemical staining using mouse mAb. A primary mAb (CMIC) against h-L-FABP (not cross-reacting to mice L-FABP) of 1:500 dilutions was applied to sections and incubated for 1 h at room temperature. The subsequent procedure of mouse sections was conducted according to the manufacturer's instructions of the Histofine Mice Stain Kit. That of human sections was followed by Vectastain ABC system (Vector Laboratories, Burlingame, CA) protocol. For substrate-chromogen reaction, diaminobenzidine tetrahydrochloride (Simple Stain DAB; Nichirei) was used following the manufacturer's protocol. Control sections were subjected to secondary antibody only (blank). Mounted preparations were examined using light microscopy (Nikon Eclipse 80i; Nikon, Tokyo, Japan). Images were captured by CCD camera (DXM1200F; Nikon).

Experiment with Hypoxic Probe

The level of the outer medulla to cortical ischemia was evaluated immunohistochemically using a hypoxic probe-1 system of pimonidazole (Chemicon, Temecula, CA). Pimonidazole was injected into mice *via* a tail vein 1 h before starting ischemia. After 30 min of ischemia, another 2 h was used for the reperfusion period. During this 2-h period, pimonidazole was reductively activated and protein adducts were generated. The specific antibody (Chemicon) raised against this particular adduct was used for detection of the hypoxic area. Mice were then killed, and their kidneys were fixed into 10% buffered formalin. Immunohistochemistry was performed following the manufacturer's protocol. For evaluation of pimonidazole, the positive area and expression of h-L-FABP in ischemic h-L-FABP-Tg kidney, staining obtained from serial sectioning, were combined using the overlay function of image software (MetaMorph 5.0; Universal Imaging, Downingtown, PA); simultaneously, the hypoxic area and L-FABP–positive area were quantified using another image software package (AIS).

Real-Time Quantitative PCR Analysis

Total RNA was extracted from the outer medulla to cortical kidney homogenates using Trizol (Invitrogen, Carlsbad, CA). In a part of the experiment, total RNA was extracted from cultured cells. To synthesize cDNA from total RNA, we used SuperScript II Reverse Transcriptase (Invitrogen). Renal mRNA levels were assessed using real-time quantitative PCR with TaqMan Universal PCR Master Mix (Applied Biosystems, Foster City, CA) and a Prism 7000 PCR system (Applied Biosystems) according to the manufacturer's instructions. Each gene and PCR primer was obtained from Assay-on-Demand (Applied Biosystems) as follows: h-L-FABP, assay ID Hs00155026_m1; and 18s ribosomal RNA, assay ID Hs99999901_s1.

Fluorescence Measurement of Intracellular ROS

The stable C57Bl/6 mice proximal tubular cell line, mProx, was obtained by the previously reported method without virus transfection.[29] Because mProx does not express L-FABP, h-L-FABP including the promoter region was transfected to mProx by FuGene 6 (Roche, Mannheim, Germany) and mProx-L was obtained. As seen in Figure 8B, mProx is stably expressing h-L-FABP. Both mProx and mProx-L were maintained by K-1 medium supplemented with ITS (BD Pharmingen, San Diego, CA), 10^{-8} M dexamethasone, 2.5 mM nicotinamide, and 10% FBS (JRH Biosciences, Lenexa, KS). Both cells were lifted with 0.05% trypsin-0.53 mM EDTA (Invitrogen) and washed, and 1.5×10^4 cells/ml suspended in 200 μl of that culture medium were seeded per well in 96-well plates (Corning, Corning, NY) in a part of the experiment. To measure intracellular ROS production, both mProx and mProx-L were changed to serum reduced (0.5% FBS) experimental medium. Both mProx and mProx-L were subjected to hypoxia for 24 h using BBL GasPak Pouch (BD Pharmingen). Cells were loaded with 10 μM CM-H_2DCFDA (Invitrogen) for 30 min at 37°C in the dark following the previously reported protocol.[13] During each experiment, fluorescence of CM-H_2DCFDA was measured on four separate cell monolayers using an excitation wavelength of 485 nm and an emission wavelength of 538 nm by a fluorescence microplate reader (fMax; Molecular Devices, Sunnyvale, CA). Nine samples were prepared for each group.

Evaluation of Clinical Outcome

To evaluate the clinical outcome in each of the 12 patients studied, we compared the parameters of the urine drained from the transplanted kidney ureter (*i.e.*, initial levels of L-FABP, NAG, and β2-microglobulin) and renal microcirculation of the transplanted kidney with the representative parameters reflecting clinical outcome, as follows: Levels of postoperative BUN and SCr, occurrence of renal replacement therapy after transplantation, and duration of hospital stay.

Statistical Analyses

Correlations between two indicators were evaluated using Spearman rank test, and $r > 0.6$ was considered a significant correlation. Differences among experimental groups were detected by one-way ANOVA using Scheffe *post hoc* analysis. Values are expressed as means $\pm$ SD; $P < 0.05$ was considered significant. Statistical analysis was performed by SAS 9.1 (SAS Institute Japan, Tokyo, Japan).

ACKNOWLEDGMENTS

Part of this study was supported by the Health and Labor Sciences Research Grants for Research on Human Genome, Tissue Engineering Food Biotechnology, MHLW, Japan (057100000661 to T.Y., E.N., Y.O., H.T., N.S., S.O., and T.S.); by the BioBank Japan Project on the Implementation of Personalized Medicine, MEXT, Japan (3023168 to E.N.); by Special Coordination Funds for Promoting Science and

Technologies, MEXT, Japan (1200015 to E.N.); and by KAKENHI, MEXT, Japan (19590935 to E.N. and T.S.).

We are grateful to Ms. Yokura, Mr. Okamoto, Dr. Fujita, Dr. Tsuji, and Ms. Maeda for skilled assistance.

DISCLOSURES

None.

REFERENCES

1. Tan NS, Shaw NS, Vinckenbosch N, Liu P, Yasmin R, Desvergne B, Wahli W, Noy N: Selective cooperation between fatty acid binding proteins and peroxisome proliferator-activated receptors in regulating transcription. *Mol Cell Biol* 22: 5114–5127, 2002
2. Chmurzynska A: The multigene family of fatty acid-binding proteins (FABPs): Function, structure and polymorphism. *J Appl Genet* 47: 39–48, 2006
3. Bennaars-Eiden A, Higgins L, Hertzel AV, Kapphahn RJ, Ferrington DA, Bernlohr DA: Covalent modification of epithelial fatty acid-binding protein by 4-hydroxynonenal in vitro and in vivo: Evidence for a role in antioxidant biology. *J Biol Chem* 277: 50693–50702, 2002
4. Wang G, Gong Y, Anderson J, Sun D, Minuk G, Roberts MS, Burczynski FJ: Antioxidative function of L-FABP in L-FABP stably transfected Chang liver cells. *Hepatology* 42: 871–879, 2005
5. Kanda T, Fujii H, Fujita M, Sakai Y, Ono T, Hatakeyama K: Intestinal fatty acid binding protein is available for diagnosis of intestinal ischaemia: Immunochemical analysis of two patients with ischaemic intestinal diseases. *Gut* 36: 788–791, 1995
6. Nakata T, Hashimoto A, Hase M, Tsuchihashi K, Shimamoto K: Human heart-type fatty acid-binding protein as an early diagnostic and prognostic marker in acute coronary syndrome. *Cardiology* 99: 96–104, 2003
7. Kamijo-Ikemori A, Sugaya T, Obama A, Hiroi J, Miura H, Watanabe M, Kumai T, Ohtani-Kaneko R, Hirata K, Kimura K: Liver-type fatty acid-binding protein attenuates renal injury induced by unilateral ureteral obstruction. *Am J Pathol* 169: 1107–1117, 2006
8. Portilla D: Energy metabolism and cytotoxicity. *Semin Nephrol* 23: 432–438, 2003
9. Yamamoto T, Tada T, Brodsky SV, Tanaka H, Noiri E, Kajiya F, Goligorsky MS: Intravital videomicroscopy of peritubular capillaries in renal ischemia. *Am J Physiol Renal Physiol* 282: F1150–F1155, 2002
10. Conger JD, Schultz MF, Miller F, Robinette JB: Responses to hemorrhagic arterial pressure reduction in different ischemic renal failure models. *Kidney Int* 46: 318–323, 1994
11. Solez K, Morel-Maroger L, Sraer JD: The morphology of "acute tubular necrosis" in man: Analysis of 57 renal biopsies and a comparison with the glycerol model. *Medicine (Baltimore)* 58: 362–376, 1979
12. Noiri E, Peresleni T, Miller F, Goligorsky MS: In vivo targeting of inducible NO synthase with oligodeoxynucleotides protects rat kidney against ischemia. *J Clin Invest* 97: 2377–2383, 1996
13. Doi K, Suzuki Y, Nakao A, Fujita T, Noiri E: Radical scavenger edaravone developed for clinical use ameliorates ischemia/reperfusion injury in rat kidney. *Kidney Int* 65: 1714–1723, 2004
14. Van Nieuwenhoven FA, Kleine AH, Wodzig WH, Hermens WT, Kragten HA, Maessen JG, Punt CD, Van Dieijen MP, Van der Vusse GJ, Glatz JF: Discrimination between myocardial and skeletal muscle injury by assessment of the plasma ratio of myoglobin over fatty acid-binding protein. *Circulation* 92: 2848–2854, 1995
15. Simon TC, Roth KA, Gordon JI: Use of transgenic mice to map cis-acting elements in the liver fatty acid-binding protein gene (Fabpl) that regulate its cell lineage-specific, differentiation-dependent, and spatial patterns of expression in the gut epithelium and in the liver acinus. *J Biol Chem* 268: 18345–18358, 1993
16. Allgren RL, Marbury TC, Rahman SN, Weisberg LS, Fenves AZ, Lafayette RA, Sweet RM, Genter FC, Kurnik BR, Conger JD, Sayegh MH: Anaritide in acute tubular necrosis. Auriculin Anaritide Acute Renal Failure Study Group. *N Engl J Med* 336: 828–834, 1997
17. Wang S, Hirschberg R: Role of growth factors in acute renal failure. *Nephrol Dial Transplant* 12: 1560–1563, 1997
18. Kamijo A, Kimura K, Sugaya T, Yamanouchi M, Hikawa A, Hirano N, Hirata Y, Goto A, Omata M: Urinary fatty acid-binding protein as a new clinical marker of the progression of chronic renal disease. *J Lab Clin Med* 143: 23–30, 2004
19. Fine LG, Bandyopadhay D, Norman JT: Is there a common mechanism for the progression of different types of renal diseases other than proteinuria? Towards the unifying theme of chronic hypoxia. *Kidney Int Suppl* 75: S22–S26, 2000
20. Kang DH, Kanellis J, Hugo C, Truong L, Anderson S, Kerjaschki D, Schreiner GF, Johnson RJ: Role of the microvascular endothelium in progressive renal disease. *J Am Soc Nephrol* 13: 806–816, 2002
21. Noiri E, Tsukahara H: Parameters for measurement of oxidative stress in diabetes mellitus: Applicability of enzyme-linked immunosorbent assay for clinical evaluation. *J Investig Med* 53: 167–175, 2005
22. Paller MS, Hoidal JR, Ferris TF: Oxygen free radicals in ischemic acute renal failure in the rat. *J Clin Invest* 74: 1156–1164, 1984
23. Noiri E, Nakao A, Uchida K, Tsukahara H, Ohno M, Fujita T, Brodsky S, Goligorsky MS: Oxidative and nitrosative stress in acute renal ischemia. *Am J Physiol Renal Physiol* 281: F948–F957, 2001
24. Takeuchi N, Ohshima S, Ono Y, Sahashi M, Matsuura O, Yamada S, Tanaka K, Kuriki O, Kamihira O: Five-year results of thoracic duct drainage in living related donor kidney transplantation. *Transplant Proc* 24: 1421–1423, 1992
25. Hashimoto Y, Nagano S, Ohsima S, Takahara S, Fujita T, Ono Y, Kinukawa T: Surgical complications in kidney transplantation: Experience from 1200 transplants performed over 20 years at six hospitals in central Japan. *Transplant Proc* 28: 1465–1467, 1996
26. Yamamoto T, Kajiya F: Intravital videomicroscopy. *Methods Mol Med* 86: 119–128, 2003
27. Kamijo A, Sugaya T, Hikawa A, Okada M, Okumura F, Yamanouchi M, Honda A, Okabe M, Fujino T, Hirata Y, Omata M, Kaneko R, Fujii H, Fukamizu A, Kimura K: Urinary excretion of fatty acid-binding protein reflects stress overload on the proximal tubules. *Am J Pathol* 165: 1243–1255, 2004
28. Doi K, Okamoto K, Negishi K, Suzuki Y, Nakao A, Fujita T, Toda A, Yokomizo T, Kita Y, Kihara Y, Ishii S, Shimizu T, Noiri E: Attenuation of folic acid-induced renal inflammatory injury in platelet-activating factor receptor-deficient mice. *Am J Pathol* 168: 1413–1424, 2006
29. Okada H, Kikuta T, Inoue T, Kanno Y, Ban S, Sugaya T, Takigawa M, Suzuki H: Dexamethasone induces connective tissue growth factor expression in renal tubular epithelial cells in a mouse strain-specific manner. *Am J Pathol* 168: 737–747, 2006

Supplemental information for this article is available online at http://www.jasn.org/.

http://www.kidney-international.org

A role of liver fatty acid-binding protein in cisplatin-induced acute renal failure

K Negishi[1], E Noiri[1], T Sugaya[2], S Li[3], J Megyesi[3], K Nagothu[3] and D Portilla[3]

[1]Department of Nephrology and Endocrinology, University of Tokyo, Tokyo, Japan; [2]CMIC Ltd, Tokyo, Japan and [3]Division of Nephrology, Department of Internal Medicine, University of Arkansas for Medical Sciences and Central Arkansas Veterans Healthcare System, Little Rock, Arkansas, USA

Previous studies from our laboratory showed that increased fatty acid oxidation by the kidney is cytoprotective during cisplatin (CP)-mediated nephrotoxicity. In this study, we determined the effects of CP and fibrates on peroxisome proliferation and the expression of liver fatty acid-binding protein (L-FABP) in normal mice, and in mice transgenically overexpressing human L-FABP (h-L-FABP). Labeling of peroxisomes demonstrated reduced peroxisomal staining in the proximal tubule of CP-treated mice compared with control mice. There was increased peroxisomal labeling in the proximal tubules of both control and CP-treated mice when either was treated with fibrate; a known peroxisome proliferator-activated receptor-α ligand. L-FABP protein expression, not detected in control or CP-treated mice, was significantly increased in the proximal tubules of fibrate-treated mice of either group. In the transgenic mice, CP increased the shedding of h-L-FABP in the urine, which was decreased by fibrate as was the acute renal failure.
A cytosolic pattern of h-L-FABP expression was found in the proximal tubules of untreated transgenic mice with a nuclear presence in CP-treated mice. Fibrate pretreatment restored the cytosolic expression pattern in CP-treated mice. Our study shows that fibrate may improve CP-induced acute renal failure due to both peroxisome proliferation and increased L-FABP in the cytosol of the proximal tubule.

Kidney International (2007) **72,** 348–358; doi:10.1038/sj.ki.5002304; published online 9 May 2007

KEYWORDS: acute renal failure; cisplatin nephrotoxicity; lipids

Correspondence: *D Portilla, Department of Medicine, University of Arkansas for Medical Sciences, Slot 501, 4301 W. Markham St, Little Rock, Arkansas 72205, USA. E-mail: portilladidier@uams.edu*

Received 17 January 2007; revised 9 March 2007; accepted 20 March 2007; published online 9 May 2007

The intracellular fatty acid-binding proteins (FABPs) belong to a super family of lipid-binding proteins with low molecular weight (14–15 kDa), which are classified according to their predominant tissue localization. There are nine different FABPs, with tissue-specific distribution that include L (liver), I (intestinal), H (muscle and heart), A (adipocyte), E (epidermal), Il (ileal), B (brain), M (myelin), and T (testis).[1] The liver isoform of FABP (L-FABP) is highly expressed in hepatocytes, where it represents 5% of the total cytosolic protein. L-FABP facilitates the cellular uptake, transport, and metabolism of fatty acids, and is also involved in the regulation of gene expression and cell differentiation.[2–5] Previous work in liver tissue has shown (1) that the level of L-FABP expression in rodent liver is regulated in concert with peroxisome proliferation and (2) that the transcription rate of L-FABP gene is regulated and induced by both fibrate hypolipidemic drugs and long-chain fatty acids, through a peroxisome proliferator-activated receptor (PPAR)-responsive element located in its promoter region.[6,7]

Although the kidney in rodents does not synthesize a significant amount of L-FABP protein,[8] recent work suggests that L-FABP under normal conditions resides in the lysosomal compartment of the proximal tubule, but also can be reabsorbed from the glomerular filtrate via megalin, a multiligand proximal tubule endocytic receptor.[9] On the other hand, the amount of L-FABP protein present in human kidney is considerably much higher than the amount of L-FABP protein present in rodent kidney tissue, and its expression is restricted to the proximal convoluted and straight tubules.[10,11] In more recent studies using human L-FABP (h-L-FABP) transgenic mice, which express higher protein levels of h-L-FABP in proximal tubules when compared with non-transgenic mice, Noiri *et al.*[12,13] demonstrated that the shedding of h-L-FABP was increased in urine obtained from mice that underwent ischemia–reperfusion injury. Immunohistochemical analysis of kidney tissue of h-L-FABP transgenic mice subjected to ischemia–reperfusion injury demonstrated increased translocation of h-L-FABP from the cytoplasm of the proximal tubule to the tubular lumen. In addition, renal function and histological scores of acute kidney injury, in h-L-FABP transgenic mice subjected to ischemia–reperfusion injury, were significantly ameliorated

when compared with wild-type mice. The role of L-FABP in acute kidney injury caused by cisplatin (CP) has not been examined previously.

In previous studies, we have documented that the inhibition of peroxisomal and mitochondrial fatty acid oxidation (FAO) observed in kidney tissue of mice undergoing ischemia–reperfusion injury and CP-induced acute renal failure (ARF) results from reduced activity of PPARα.[14–20] Failure to oxidize long-chain fatty acids and long-chain acylcarnitines during ARF results in their accumulation and cellular toxicity, which further contributes to proximal tubule cell death.[21,22] In a recent metabolomic study,[23] we found that CP-mediated nephrotoxicity was accompanied by increased serum levels of nonesterified fatty acids and triglycerides, as well as increased accumulation of nonesterified fatty acids and triglycerides in kidney tissue. We also observed that the administration of fibrate, a known PPARα ligand, before ARF (1) prevented the inhibition of FAO and the accumulation of nonesterified fatty acids and triglycerides in kidney tissue, and (2) ameliorated apoptotic and necrotic proximal tubule cell death, which resulted in significant protection of renal function only in PPARα wild-type mice, and not in PPARα null mice.[17–20] Altogether, these previous observations from our laboratory suggest that increased FAO, via PPARα activation, plays a significant role in the observed cytoprotection by fibrates in CP-mediated nephrotoxicity. The cellular targets by which increased PPARα activity in kidney tissue prevents ARF after CP exposure are not currently known.

In these studies, we investigated the contribution of peroxisome proliferation and L-FABP protein expression to the cytoprotective effect of fibrates in the CP model of ARF. For these studies, we used sv-129 mice as well as h-L-FABP transgenic mice. We examined the effects of CP + fibrate on L-FABP expression in kidney tissue and on the shedding of urinary h-L-FABP. In addition, we performed immunohistochemical studies to examine the effects of CP + fibrate on peroxisome proliferation, and the intracellular localization of L-FABP in kidney tissue, and correlated with effects on renal function.

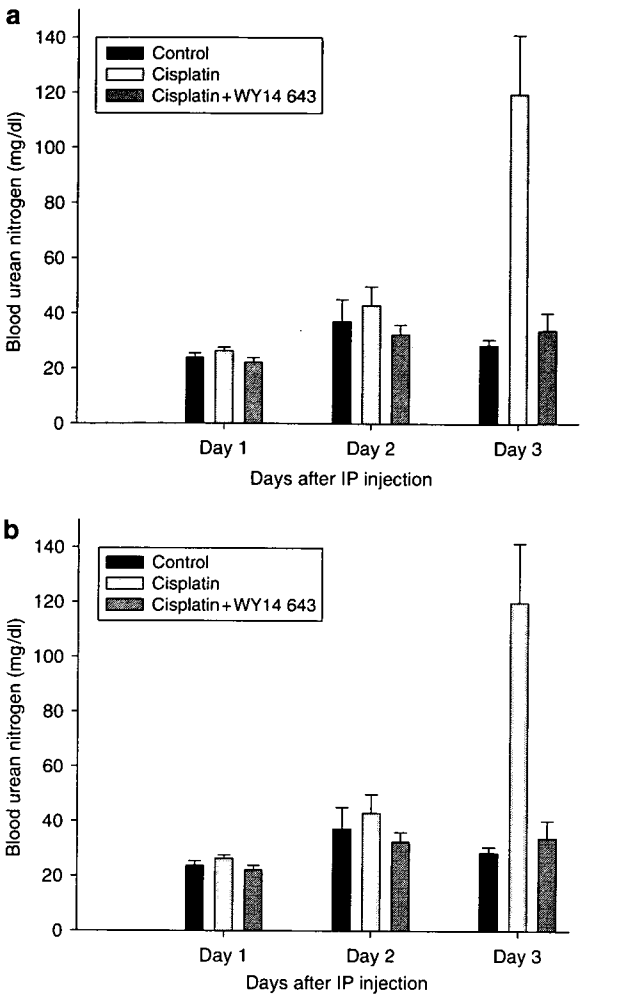

Figure 1 | Effect of fibrate WY-14643 (WY) on renal function in mice after single dose of CP. Mice were fed with either a regular diet or a diet containing 0.1% WY for 7 days before CP administration, as described in Materials and Methods. BUN and creatinine levels were measured at days 1, 2, and 3 after saline (control)-, CP-, or CP + WY-treated mice. Bars correspond to mean ± s.e. of at least six independent experiments under each condition. Changes in (**a**) BUN and (**b**) creatinine levels, respectively, after saline or CP administration in PPARα wild-type mice. $^*P < 0.005$ when animals were compared with control by unpaired Student's *t*-test.

RESULTS

Studies in sv129 mice

Protective effects of PPARα ligand on CP-induced ARF. Kidney function was monitored by measuring blood urea nitrogen (BUN) and serum creatinine for 3 days after intraperitoneal injection of saline (groups: control and WY) or CP (groups: CP and CP + WY). Figure 1a and b present the changes on BUN and creatinine in mice treated with saline (control), CP, and with WY in the presence of CP. Mice treated with a regular diet and CP developed ARF at day 3 (BUN increased from 28 to 135 and creatinine increased from 0.2 to 1.2 mg/dl). The group of mice that received the WY diet and CP did not develop significant ARF when compared with mice treated with CP alone (BUN increased from 24 on day 1 to 32 and creatinine was unchanged at 0.2 mg/dl after 3 days of CP administration). By contrast, the protective effect of the ligand was lost in PPARα null mice treated with CP (data not shown). PPARα null mice pretreated with a fibrate diet before CP administration developed ARF at day 3. BUN increased from 30 at day 1 to 186 at day 3 and creatinine increased from 0.3 at day 1 to 1.5 mg/dl at day 3.

Effects of CP + fibrates on the expression of 70-kDa peroxisomal membrane protein and peroxisomal matrix protein catalase. We examined by Western blot analysis whether CP or fibrate (WY) treatment had an effect on protein levels of 70-kDa peroxisomal membrane protein (PMP70) or catalase. As shown in Figure 2a, CP-treated mice exhibited a time-dependent reduction in PMP70 protein levels. PMP70

protein levels were reduced by 50% at day 2 and by 75% at day 3 after CP injection. As our studies have shown that the use of PPARα ligand-like fibrates prevent the development of CP-induced proximal tubule cell death by preventing the inhibition of FAO,[14,17] we next examined the effect of fibrate on PMP70 protein levels. As shown in Figure 2b, at day 3 after CP injection, there was a 75% reduction in PMP70 protein levels. In contrast, the group of mice that received the diet containing the fibrate + CP exhibited increased levels of PMP70 by 1.5-fold for fibrate alone, and 1.5-fold for fibrate + CP-treated mice when compared with control untreated mice. We also measured by Western blot analysis protein levels of catalase, a peroxisomal matrix protein. CP at day 3 caused a 30% reduction in expression of a 60-kDa protein corresponding to catalase, and fibrate + CP significantly increased catalase protein expression to levels similar to the ones observed in control untreated mice, as shown in Figure 3.

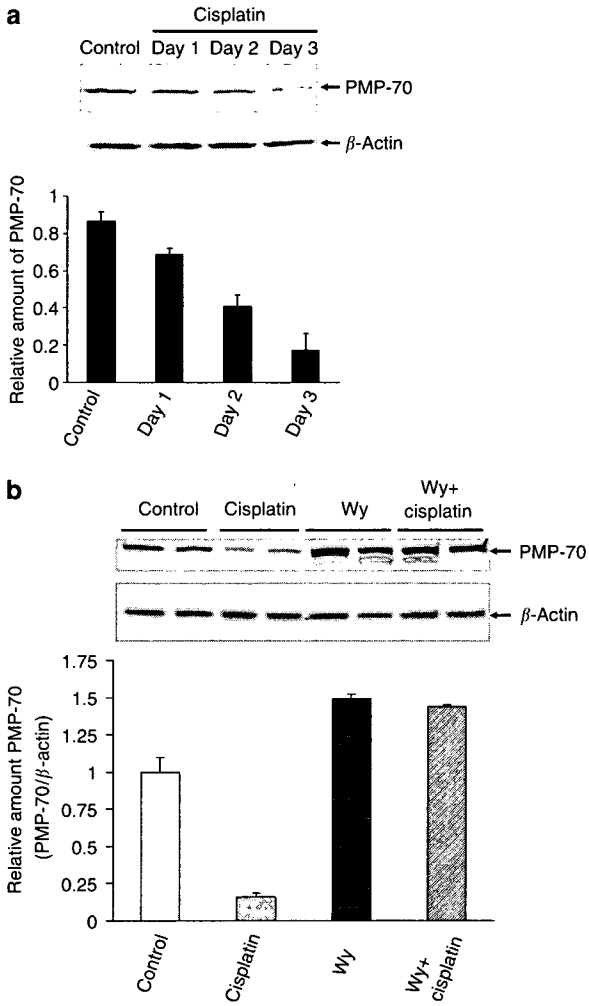

Figure 2 | Effect of fibrate and cisplatin on PMP70 expression in kidney tissue. (**a**) Time course of the effect of CP on PMP70 protein expression in kidney tissue. Mice were administered saline (control) or CP (20 mg/kg body weight) by a single intraperitoneal injection. Western blot analysis of kidney tissue homogenates at days 1, 2, and 3 after CP injection using a PMP70 antibody as described in Materials and Methods. Bars correspond to mean ± s.e. of at least three independent experiments under each condition. (**b**) Effect of fibrate (WY) and CP on PMP70 protein expression. Mouse kidney tissue homogenates were prepared from animals subjected to four experimental conditions, and Western blots were performed as described in Materials and Methods. PMP-70 protein levels were normalized using β-actin as internal control. Bars correspond to mean ± s.e. of at least three independent experiments under each condition.

Image analysis of quantum dot peroxisome fluorescence from kidneys of fibrate-treated mice. To determine the effects of CP + fibrate on peroxisome proliferation, we used a recently developed method for immunofluorescent staining of peroxisomes and quantification of peroxisome fluorescence using an antibody to the PMP70 coupled with fluorescent nanocrystals, Quantum Dots™.[24] The quantum dot peroxisome fluorescence information is contained in the red channel of the RGB image, so quantification is performed in the red channel using a confocal microscope. As shown in Figure 4a, the pixel intensity of red/orange quantum dots was predominantly observed in the proximal tubules of control untreated mice ($15 \times 10^3 \pm 1406$ pixel fluorescent units) and was significantly elevated in fibrate (WY)-treated mice ($21 \times 10^3 \pm 1256$ pixel fluorescent units; Figure 4b). The intensity of pixels was significantly reduced in CP-treated animals ($1.7 \times 10^3 \pm 803$ pixel fluorescent units; Figure 4c) when compared with fibrate (WY) + CP-treated mice $19 \times 10^3 \pm 1167$ pixel fluorescent units; Figure 4d). Figure 4e summarizes data obtained from four separate experiments.

Effect of CP on mouse L-FABP mRNA levels in kidney tissue of sv129 mice. We next examined the effects of CP on mRNA expression of mouse L-FABP (mL-FABP) in kidney tissue of sv129 mice. As shown in Figure 5, by real-time reverse transcriptase-polymerase chain reaction quantitative analysis, after 3 days of CP injection, there was a mild (1.5–1.8-fold)

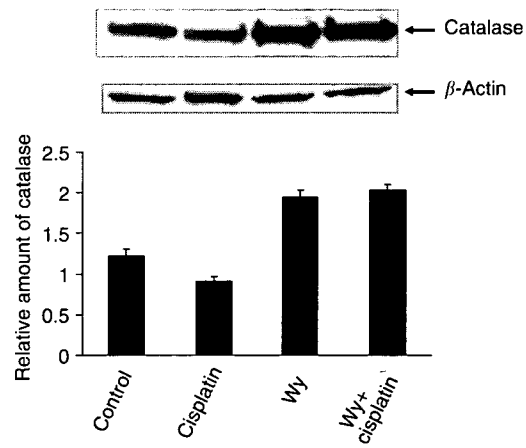

Figure 3 | Effect of fibrate (WY) and CP on catalase protein expression. Mouse kidney tissue homogenates were prepared from animals subjected to four experimental conditions, and Western blots were performed as described in Materials and Methods. Catalase protein levels were normalized using β-actin as internal control. Bars correspond to mean ± s.e. of at least three independent experiments under each condition.

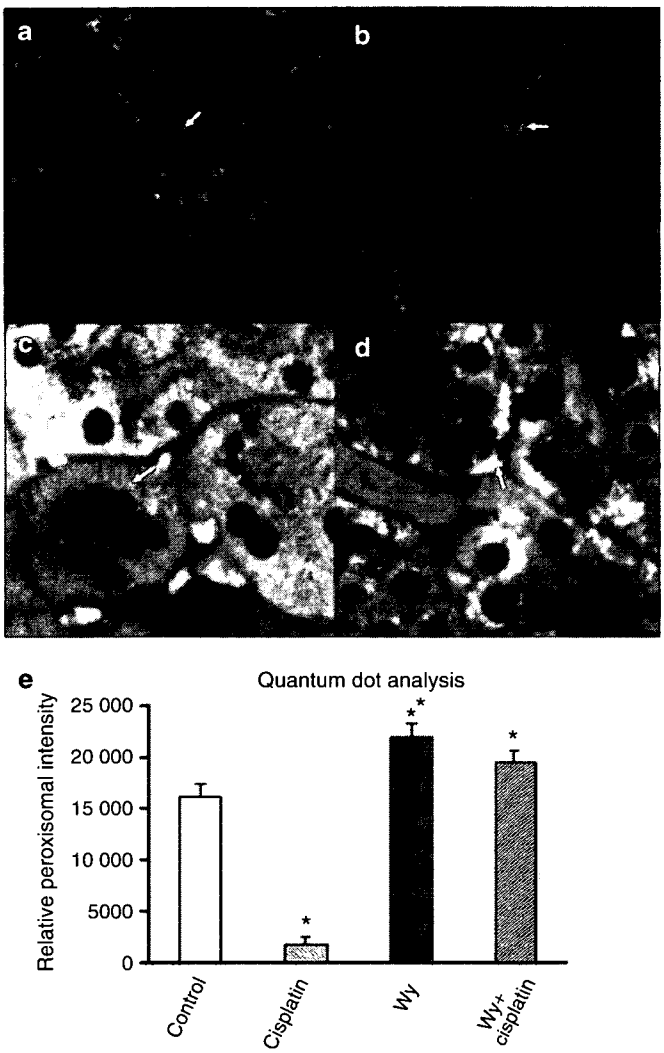

Figure 4 | Effect of fibrate (WY) and CP on peroxisomal distribution. (**a**) Mouse kidney sections from animals subjected to four experimental conditions (**a**) control, (**b**) fibrate (WY), (**c**) CP, and (**d**) WY + CP were stained with PMP70 antibody as described in Materials and Methods. (**e**) Quantitative analysis of pixel densities of the peroxisomal population present in the four experimental conditions was performed as described in the Materials and Methods section. Bars correspond to mean ± s.e. of at least four independent experiments under each condition.

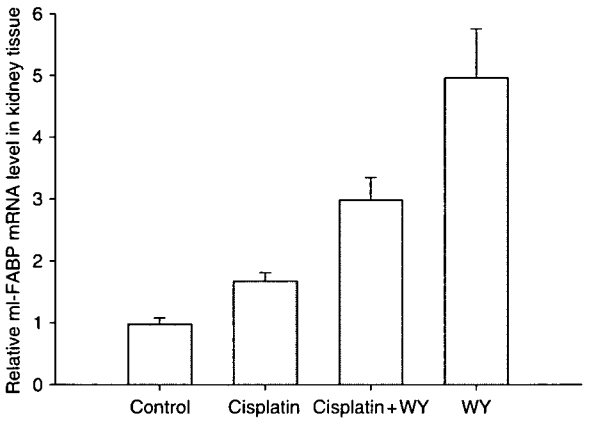

Figure 5 | Effect of CP and fibrate on mL-FABP mRNA levels in SV-129 wild-type mice. Mice that received either a normal diet or a diet containing fibrate (WY) for 7 days were injected with saline (control) or CP and then killed at the indicated times. Levels of mL-FABP mRNA was measured by real-time reverse transcriptase-polymerase chain reaction as described in Materials and Methods. Figure shows relative mL-FABP gene expression in saline (control), CP-, CP + fibrate-, and fibrate-treated mice normalized by 28S rRNA expression. Values are mean ± s.e. mRNA levels. Data were obtained from at least three independent experiments.

increase in the mL-FABP mRNA levels when compared with saline-treated mice. In kidney tissue of sv129 mice treated with CP + fibrate, there was a 3.0-fold increase on L-FABP mRNA levels ($P<0.01$), and fibrate alone upregulated L-FABP mRNA expression by fivefold ($P<0.01$) when compared with saline-treated mice.

Fibrate increases L-FABP protein expression in kidney tissue of PPARα wild type but not on PPARα null mice. Using antibodies that recognize mL-FABP and kidney tissue isolated from sv129 mice treated with CP + fibrate (WY), we found that protein expression of mL-FABP, which was not detected in kidney tissue of untreated or CP-treated sv129 mice, was significantly induced in the proximal tubules of PPARα wild-type mice treated with the fibrate, in the absence and presence of CP. Western blot analysis of mL-FABP, shown in Figure 6a, demonstrates that L-FABP protein was not detected in control or CP-treated sv129 mice. However, treatment of sv129 mice with PPARα ligand WY led to a rapid increase in the expression of mL-FABP. Even though CP treatment slightly reduced expression of L-FABP protein level, it remained significantly elevated in the presence of PPARα ligand WY. By contrast, mL-FABP expression was not detected in kidney tissue of PPARα null mice treated with fibrates, where we did not see protection from CP-induced ARF, as shown in Figure 6b.

Immunohistochemical localization of mL-FABP. Immunohistology of normal mouse kidney cortex demonstrated no positive L-FABP staining (Figure 7a). As shown in Figure 7b, L-FABP is highly expressed in Bowman capsule and early proximal tubule cells of WY-treated animals. In fibrate-treated sv129 mice, a strongly positive staining was seen in the cytosol and perinuclear localization. Only occasional, single cell-positive staining could be seen in CP-treated animals in intact proximal tubules (Figure 7c). Similarly to the WY-treated animals, the positive L-FABP immunoreactivity was detected in Bowman capsule and early proximal tubule cells in kidneys from WY + CP-treated mice (Figure 7d). There was no positive staining in glomeruli and distal nephron segments.

Studies in h-L-FABP transgenic mice

Effects of CP + fibrate on renal function in h-L-FABP transgenic mice. To further examine the regulation of L-FABP expression in mouse kidney tissue, we used h-L-FABP transgenic mice. These mice express higher levels of h-L-FABP protein

in the cytosolic compartment of the proximal tubule when compared with non-transgenic mice, and do not exhibit a particular histologic or functional renal phenotype. In previous published studies using these same h-L-FABP transgenic mice, Noiri[13] and Kamijo *et al.*[25] demonstrate that acute kidney injury due to ischemia–reperfusion injury and unilateral ureteral obstruction was significantly ameliorated when compared with wild-type non-transgenic mice. CP was administered at a dose of 20 mg/kg body weight, and fibrate was administered as a diet containing 0.5% bezafibrate (Bz) for 7 days before the administration of CP. Figure 8a and b present the changes on BUN and creatinine in h-L-FABP transgenic mice treated with saline (control), CP, and with Bz in the absence and presence of CP. Mice treated with a regular diet and CP developed ARF at day 3 (BUN increased from 24 to 143 and creatinine increased from 0.15 to 1.50 mg/dl). The group of mice that received the Bz diet and CP were significantly protected from CP nephrotoxicity, when compared with mice treated with CP alone (BUN increased from 24 to 62 and creatinine increased from 0.15 to 0.47 mg/dl).

Effect of CP + fibrate on shedding of urinary h-L-FABP. In h-L-FABP transgenic mice treated with CP, analysis of urinary h-L-FABP protein by enzyme-linked immunosorbent assay demonstrated a time-dependent increase in the shedding of urinary h-L-FABP protein, which was detected within the first 24 h after CP administration ($n = 12$). Figure 9 shows the time course of shedding of urinary h-L-FABP after CP or

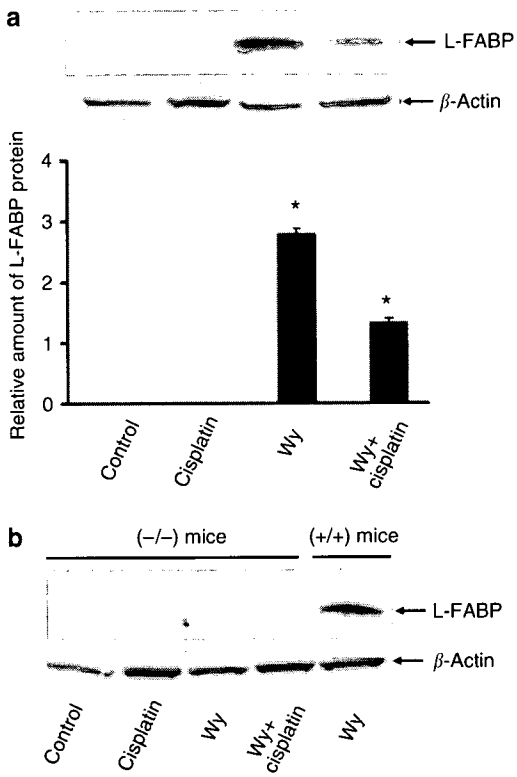

Figure 6 | Effect of CP and Wy on L-FABP protein levels in SV-129 wild-type (+/+) and PPARα null (−/−) mice. (**a**) Effect f of CP and WY on L-FABP protein levels in SV-129 wild-type (+/+) mice. The immunoblot analysis of mouse kidney tissue homogenates from four different experimental conditions was performed as described in Materials and Methods. β-Actin antibody was used as an internal control for normalizing the L-FABP protein levels. Bars correspond to mean ± s.e. of at least three independent experiments under each condition. *$P < 0.005$ when animals were compared with control by unpaired Student's *t*-test. (**b**) Effect f of CP and fibrate on L-FABP protein levels in sv-129 PPARα knock out (−/−) mice. The immunoblot analysis of mouse kidney tissue homogenates from four different experimental conditions was performed as described in Materials and Methods. Kidney homogenate from wild-type mice treated with fibrate (WY) was run as positive control for L-FABP protein. β-Actin antibody was used as an internal control for normalizing the L-FABP protein levels.

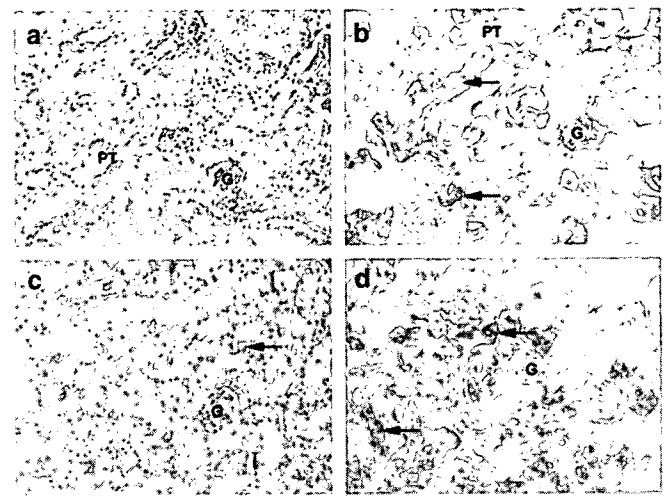

Figure 7 | Immunolocalization of mL-FABP. Representative picture of kidney sections from (**a**) control-, (**b**) fibrate (WY)-, (**c**) CP-, and (**d**) WY + CP-treated mice stained with anti-mL-FABP antibody. Positive immunostaining was apparent only in fibrate and fibrate + CP-treated mice predominantly in proximal tubules (PT) of the outer cortex (arrows). Original magnification × 122.

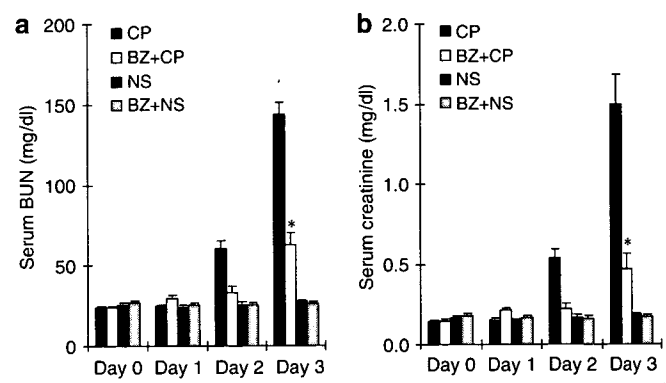

Figure 8 | Effect of Bz on renal function in h-L-FABP transgenic mice after single dose of CP. Mice were fed with either a regular diet or a diet containing 0.1% Bz for 7 days before CP administration, as described in Materials and Methods. BUN and creatinine levels were measured at days 1, 2, and 3 after saline control (NS)-, CP (CP)-, CP + Bz (CP + BZ)-, or saline + Bz (BZ + NS)-treated mice. Bars correspond to means ± s.e. of at least 10 independent experiments under each condition. (**a**) Changes in BUN and (**b**) creatinine levels, respectively, after saline or CP administration in PPARα wild-type mice. *$P < 0.05$ when CP + Bz group was compared with CP alone group by unpaired Student's *t*-test.

saline administration. In CP-treated h-L-FABP transgenic mice, urinary h-L-FABP levels increased by 100-fold at day 1 after CP injection, from baseline levels of 13.6 $\mu g/g$ creatinine in saline-treated mice to 1334.9 $\mu g/g$ creatinine in CP-treated mice. At 3 days after CP injection, urinary h-L-FABP levels did increase by 647-fold from baseline level of 12.9–8422 $\mu g/g$ creatinine. Urinary levels of h-L-FABP were significantly reduced in the Bz + CP-treated group when compared with CP-treated mice (urinary h-L-FABP levels were reduced from 8422 to 1120 $\mu g/g$ creatinine at day 3 after CP administration). Statistical significance between different time points in the same group was evaluated by paired *t*-test, and the statistical significance between two separate groups was evaluated by analysis of variance. Our results suggest that the increased shedding of h-L-FABP protein in urine samples obtained from CP-treated h-L-FABP transgenic mice precedes changes in serum creatinine or BUN, which were not detected until 2–3 days after CP administration as shown in Figure 8. Our results also show that very small amounts of urinary h-L-FABP are also shed by the administration of a PPARα ligand.

Immunohistochemical localization of h-L-FABP in h-L-FABP transgenic mice. There was no positive immunoreactivity for h-L-FABP in kidneys from control C57Bl wild-type non-transgenic mice (Figure 10a). Untreated h-L-FABP transgenic animals showed strong positive staining in the cytoplasm of early (S1 and S2) segments of proximal tubules, with occasional strong perinuclear appearance (Figure 10b). In kidney tissue of h-L-FABP transgenic mice, CP administration caused a positive nuclear staining for h-L-FABP in the epithelium of Bowman capsule and early (S1 and S2) segments of proximal tubules (Figure 10c). The Bz + CP-treated mice showed strong cytoplasmic staining in proximal tubules of the deep cortex (S3 segment; Figure 10d). Glomeruli and distal nephron segment were mainly negative.

Morphologic changes of kidneys from h-L-FABP transgenic mice after CP treatment with and without Bz pretreatment. CP-treated h-L-FABP transgenic mice showed severe tubular necrosis in the outer cortex (primarily S1 and S2 segments of proximal tubule). Necrosis was accompanied by loss of brush border; tubular dilatation, and numerous casts (Figure 11a). Necrosis was markedly reduced in h-L-FABP transgenic animals, which were pretreated with Bz before CP administration (Figure 11b). Proximal tubules in the corticomedullary junction (primarily S3 segments of proximal tubule) were dilated, contained periodic acid-Schiff (PAS)-positive proteinous casts, and their cytoplasm was filled with PAS-positive droplets (Figure 11c). Few animals showed signs of mild to rarely moderate degree of necrosis and tubular dilatation, loss of brush border, cast formation, which were occasionally present in the outer cortex. Proximal tubules in the corticomedullary junction had no signs of dilatation, loss of brush border, and cast formation. The PAS-positive droplets present in the CP-treated mice were missing after Bz pretreatment (Figure 11d). Interstitial inflammation, edema, red blood cell extravasation, or distal nephron segment damage were not seen. Morphologic changes were quantified and the results are shown in Figure 11e.

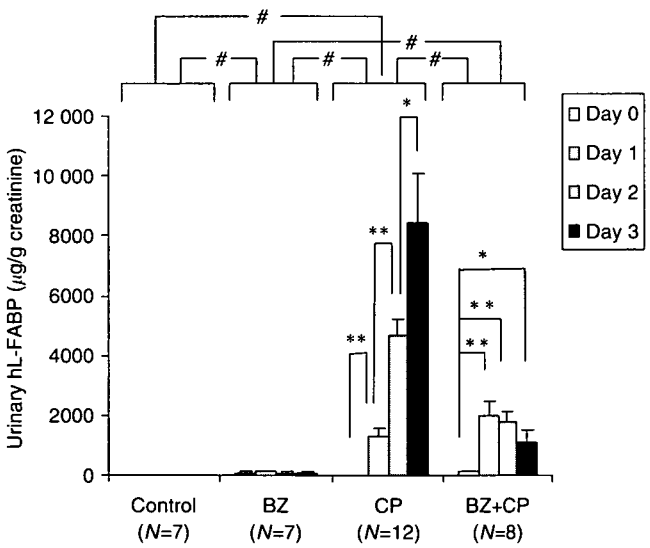

Figure 9 | Effect of BZ on urinary h-L-FABP levels after single dose of CP. Urinary h-L-FABPlevels were measured at days 1, 2, and 3 after saline control (NS)-, CP (CP)-, CP + BZ (CP + BZ)-, or saline + Bz (BZ)-treated mice by enzyme-linked immunosorbent assay as described in Materials and Methods. * Represents $P<0.05$ when urinary h-L-FABP levels were compared at day 3 and day 2 after CP administration. ** Represents $P<0.05$ when urinary h-L-FABP levels were compared at day 2 versus day 1 and day 0, and # represents $P<0.05$ when urinary h-L-FABP levels were compared among all the four groups. Bars correspond to mean ± s.e. of at least seven independent experiments under each condition.

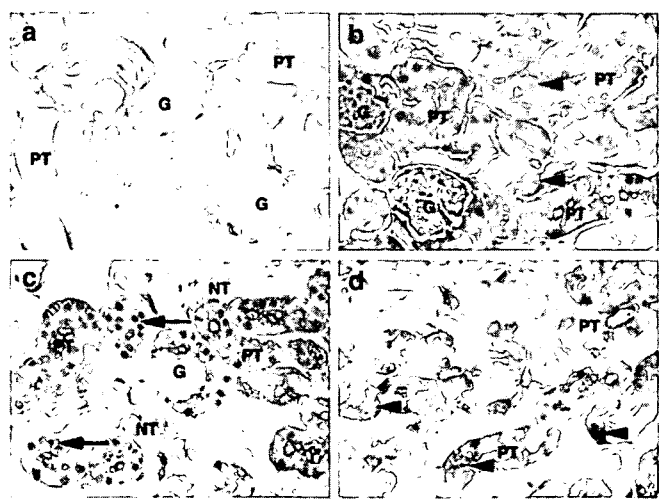

Figure 10 | Immunolocalization of h-L-FABP in h-L-FABP transgenic mice. (**a**) There was no positive immunoreactivity for h-L-FABP in kidneys from control C57Bl wild-type non-transgenic mice. (**b**) Untreated h-L-FABP transgenic animals showed strong positive staining in the cytoplasm of early (S1 and S2) segments of proximal tubules (PT). (**c**) CP administration caused a positive nuclear staining for h-L-FABP in the epithelium of Bowman capsule and early (S1 and S2) segments of proximal tubules (PT) (arrows). (**d**) The Bz + CP-treated mice showed strong cytoplasmic staining in proximal tubules (PT) of the deep cortex (S3 segment) (arrows). Glomeruli (G) and distal nephron segment were mainly negative.

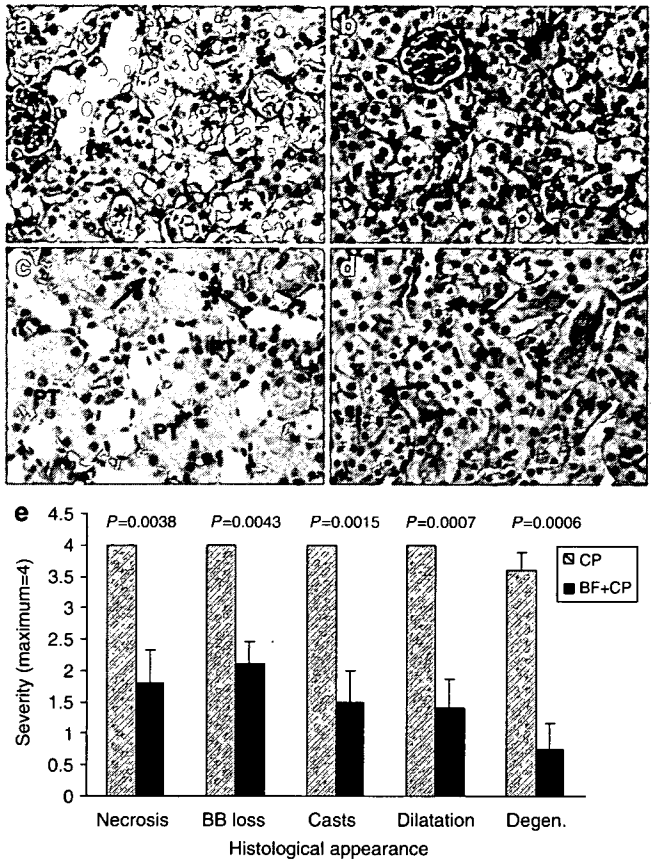

Figure 11 | Effect of Bz on kidney morphology in h-L-FABP transgenic mice after single dose of CP. Kidney morphology of h-L-FABP transgenic mice after 72 h of (**a** and **c**) CP exposure and after treatment with (**b** and **d**) Bz + CP. Severe tubular necrosis was seen in the proximal tubules (S1 and S2) of the outer cortex of (**a**) CP-treated mice (*). Bz significantly ameliorated necrosis of proximal tubules (PT) caused by (**b**) CP injection. Proximal tubules of the deep cortex (S3 segment) (PT) showed PAS-positive droplet accumulation in their cytoplasm in (**c**) CP-treated mice (arrows), which was ameliorated by (**d**) Bz pretreatment (arrows). (**e**) Quantitative evaluation of morphologic kidney damage of h-L-FABP transgenic mice after CP and Bz + CP. Values are expressed as relative severity on a scale from 0 to 4 and represent mean ± s.e. of kidney sections from at least eight mice for each experimental condition. Morphology was scored according to proximal tubule necrosis (Necrosis), brush border loss (BB Loss), cast formation within tubules (Casts), tubule dilation (Dilatation), and tubular degeneration (Degen). Statistically significant differences ($P < 0.05$) are indicated.

DISCUSSION

In this study, we demonstrate that CP causes a significant reduction in the peroxisome population of the proximal tubule determined by reduced protein expression of PMP70, and by quantification of peroxisomes using quantum dot technique. Our findings in the CP model of ARF are in agreement with findings described in the ischemia–reperfusion model of ARF, where a significant loss of catalase and fatty acid β-oxidation enzymes were accompanied by reduced number of peroxisomes in kidney tissue.[26] The mechanisms responsible for the degradation of peroxisomal proteins during ARF are unclear, but could involve autophagy, a global process by which intracellular components including soluble proteins and organelles, are degraded in lysosomes.[27–29] The presence of lysosomes containing microautophagic vacuoles has been reported previously in rat proximal tubules of animals treated with vinblastine;[30] however, the pathogenic role of these structural alterations in CP-mediated ARF remains to be defined.

Our studies showing a PPARα ligand-like fibrate increases the expression of peroxisomal proteins in mouse kidney tissue suggest that the presence of increased peroxisome proliferation in the proximal tubule is associated with cytoprotection. Peroxisome proliferation can also be seen in liver tissue of rats treated with hypolipidemic drugs such as fibrates, and it is accompanied by increased FAO.[31] Peroxisomes are organelles bound by a single membrane that are involved in metabolic processes including peroxide-based respiration, oxidative degradation of fatty acids and purines, and synthesis of plasmalogen and bile acids.[32,33] FAO is an important source of energy, especially during fasting, diabetes, or ARF.[34] Although mitochondria are considered the primary site for β-oxidation of fatty acid for energy utilization, it is now well established that peroxisomes play a key role in the metabolism of a variety of lipids such as very long-chain fatty acids, branched-chain fatty acids, dicarboxylic acids, prostaglandins, leukotrienes, thromboxanes, and pristanic acid.[35] In addition, the functional importance of peroxisomes is underscored by the severity of peroxisomal disorders such as Zellweger syndrome, X-linked adrenoleukodistrophy, and Refsum disease.[36]

Role of L-FABP in CP-induced ARF

Our study is the first one to examine the role of L-FABP in the model of CP-induced ARF. The family of fatty acid-binding proteins, which was initially discovered in 1972[37] is composed of small cytosolic proteins that are part of a conserved multigene family of intracellular lipid-binding proteins with molecular masses around 15 kDa. Two distinct isoforms of FABPs are expressed in kidney tissue the heart isoform, which is expressed in distal tubules and the liver (L-FABP) isoform, which is expressed in the proximal tubule.[38] FABPs are involved in the transport of free fatty acids from the plasma membrane to sites for oxidation (mitochondria and peroxisomes), sites for esterification into triacylglycerols or phospholipids, and the nucleus for gene regulation. Liver-type FABP found in kidney proximal tubules binds with other hydrophobic molecules such as lysophospholipids, eicosanoids, bile acids, bilirubin, heme, and hypolipidemic drugs,[39–41] and thus protects cellular structures from damage by an excess of these amphipatic molecules. Early studies by Gordon *et al.*[8] using transgenic mice to map *cis*-acting elements in the L-FABP gene indicated that nucleotides −4000 to +21 of mL-FABP contain orientation-independent suppressor sequences, which can make L-FABP to remain silent for at least the first year of postnatal life in renal proximal tubular cells of Sprague–Dawley rats and C57Bl/6 mice. We find that although L-FABP mRNA levels were slightly elevated in kidney tissue of CP-treated sv129 mice,

L-FABP protein was not found increased in kidney tissue of wild-type sv129 mice by either Western blot analysis or immunohistochemical studies. In contrast, treatment with fibrate significantly increased the expression of L-FABP protein when compared with untreated mice, and L-FABP was predominantly localized in the proximal tubule of sv-129 wild-type mice, and absent in PPARα null mice, demonstrating that the increased expression of L-FABP in kidney tissue of sv129 depends on having an intact PPARα gene.

Our studies using h-L-FABP transgenic mice to examine the pathophysiologic mechanisms involved in CP-induced ARF did allow us to uncover some important observations, which were not readily apparent when we examined kidney tissue of sv129 mice exposed to CP. The first one is that CP causes a translocation of h-L-FABP protein from the cytosolic to the nuclear compartment of proximal tubules, as shown by our immunohistochemistry studies. The effects of CP in the cellular localization of h-L-FABP could not be studied in sv129 mice because these mice do not express significant amounts of L-FABP protein. It is unclear at the moment the mechanisms that could account for the observed changes in cellular localization of h-L-FABP during CP treatment; however, future studies using immunoprecipitation and/or immunofluorescence localization using either intact kidney tissue of h-L-FABP transgenic mice or proximal tubules derived from these mice could provide additional information regarding the cellular processes and potential protein(s) involved in the regulation and/or cellular translocation of h-L-FABP during proximal tubule cell injury.

Second important observation in h-L-FABP transgenic mice was that h-L-FABP protein was shed into the urinary space early in the course of CP-induced kidney injury. Our studies using enzyme-linked immunosorbent assay methods to measure h-L-FABP protein levels allowed us to detect early shedding of h-L-FABP during the first 24 h of CP exposure, which precedes the rise on serum BUN and creatinine not detected until after 48–72 h of CP exposure. These studies suggest that shedding of h-L-FABP could represent an early urine biomarker of CP-mediated nephrotoxicity. Recently Dr Noiri and Dr Sugaya from the University of Tokyo using the model of human kidney transplantation, and more recently h-L-FABP transgenic mice and the model of 30-min ischemia–reperfusion injury demonstrated that reduced pericapillary blood flow detected by intravital CCD system was closely correlated with ischemic time of transplanted kidney. Interestingly, these investigators also detected the translocation of h-L-FABP protein from the cytoplasm of the proximal tubule to the tubular lumen by immunohistochemistry.[13] The mechanisms by which h-L-FABP is shed into the urinary space are currently unknown, but could involve disruption by CP of proximal tubule endocytic mechanisms via megalin receptor. A recent study documented that L-FABP is localized to the lysosomal compartment of the proximal tubule, but also reabsorbed from the glomerular filtrate via megalin receptor-mediated endocytosis.[9] In addition, studies using kidney-specific megalin receptor knockout mice suggest that other lipid-binding proteins such as apolipoprotein M, which is also reabsorbed in the proximal tubule via megalin receptor-mediated endocytosis, is also shed into the urinary space.[42] Our most recent findings of increased shedding of apolipoprotein M in mice that received CP suggest that disruption of megalin receptor-mediated endocytosis by CP could represent one of the mechanisms by which h-L-FABP protein and other lipocalins could be shed into the luminal space during ARF.

Third important observation made in h-L-FABP transgenic mice was that fibrate pretreatment prevented CP-mediated shedding of urinary h-L-FABP, CP-mediated translocation of proximal tubule h-L-FABP from the cytosol to the nuclear compartment, and also significantly ameliorated CP-induced acute kidney failure by reducing necrosis, brush border loss, and other parameters of proximal tubule cell injury. The increased cytosolic localization of h-L-FABP in proximal tubules of fibrate-treated mice is consistent with recent observations made in Sprague–Dawley rats treated with fibrates, where the authors demonstrated the presence of L-FABP in the matrix of liver peroxisomes.[5] The induction of peroxisomal L-FABP in rat liver tissue was accompanied by increased binding to oleic acid and cisparinaric acid, and increased β-oxidation of palmitoyl CoA and acyl CoA esterase activity, indicating that this protein modulates the function of peroxisomal lipid-metabolizing enzymes.

Altogether, our results underscore the participation of peroxisomes in the pathophysiology of CP-mediated nephrotoxicity, and the protective role of their induction via fibrates in limiting proximal tubule cell death and organ dysfunction. However, it is difficult to dissect out a single role of peroxisomes in the prevention of CP-mediated organ dysfunction, since fibrates via PPARα activation induce not only peroxisomal proteins, but also affect the transcription of other genes such as those of mitochondrial and microsomal enzymes as well. Furthermore, our previous studies also suggest a protective role of PPARα ligands on renal function by preventing not only inflammation,[19] but also by reducing systemic and renal alterations in glucose and lipid metabolism caused by CP.[23] In summary, our studies show that fibrate-mediated amelioration of CP-induced ARF is accompanied by both peroxisome proliferation as well as an increased expression of cytosolic L-FABP in the proximal tubule. The finding of an increased shedding of urinary h-L-FABP before serum creatinine rises suggests that h-L-FABP could be considered as an early biomarker of CP-mediated acute kidney injury.

MATERIALS AND METHODS

Animal model of CP-induced ARF

Experimental ARF was induced in 8-to 10-week-old male mice (strain Sv129) using CP administration. The animals used in these studies (IACUC protocol no. 2-03-1) were housed at the Veterinary Medical Unit (Central Arkansas Veterans Health Care System, Little Rock, AR, USA). When appropriate, animals were painlessly killed according to methods of euthanasia approved by the Panel on Euthanasia of the American Veterinary Medical Association. The

group of sv129 mice used for these experiments were maintained on standard chow and as indicated, a group of animals was fed with a special diet containing fibrate compound WY-14643 (WY) (1% wt/wt) for 7 days before the induction of ARF. CP was administered to sv129 mice by a single intraperitoneal injection of 20 mg/kg body weight. Engineering of h-L-FABP transgenic mice has been detailed elsewhere.[24] Briefly, genomic DNA of h-L-FABP, including its promoter region (13 kb) was microinjected into fertilized eggs obtained from C57/BL6 and CBA mice; ICR mice were used as transfected-egg recipients. The resultant transgenic mice were backcrossed for more than nine generations onto C57/BL6 mice to obtain homozygous mutant mice on an inbred background. Only heterozygous h-L-FABP transgenic mice were used in this experiment. Male h-L-FABP transgenic mice weighing 25–30 *g* were fed with standard chow diet or with a special diet containing Bz (0.5% wt/wt) for 7 days before the induction of ARF. CP was administered by a single intraperitoneal injection of 20 mg/kg body weight. After the induction of renal failure, the animals were returned to their cages and allowed free access to food and water. H-L-FABP transgenic mice were kept in glass-shielded metabolic cages (Metabolica; Sugiyamagen, Tokyo, Japan) until killing, and urine was serially collected at each 24 h interval. To measure changes in creatinine and BUN, blood was drawn from each tail vein at 0, 24, 48, and 72 h after CP administration. Serum creatinine was measured using a combined enzymic-Jaffe method.[42]

Real-time quantitative reverse transcriptase-polymerase chain reaction analysis

Mice were killed following previously described experimental conditions, and the kidneys were rapidly snap-frozen in liquid nitrogen and stored at −75°C. Total RNA was extracted with TRIzol Reagent (Invitrogen Corporation, Carlsbad, CA, USA) according to the manufacturer's directions. Total RNA extract was treated with RQ1 RNase-free DNase (Promega Corporation, Madison, WI, USA) before reverse transcription. Reverse transcription reaction was performed at 42°C for 50 min in a total volume of 20 μl containing 1 μg RNA, 0.5 μg of oligo $(dT)_{12-18}$, 200 U of superscript II RNase H reverse transcriptase (Invitrogen Life Technologies). Subsequently, reverse transcriptase was inactivated by incubation at 70°C for 15 min, followed by treatment with RNase H at 37°C for 30 min. Real-time polymerase chain reaction was performed using a DNA Engine OPTICON 2 continuous fluorescence detector (MJ Research Inc., Waltham, MA, USA) with SYBR Green I technology. In each experiment, triplicates of 50 ng cDNA (total RNA equivalent) of samples were amplified in a 50 μl reaction containing 1 × iQ™ SYBR Green Supermix (Bio-Rad Laboratories, Hercules, CA, USA). The real-time polymerase chain reaction conditions are 1 cycle at 50°C for 2 min followed by 1 cycle at 95°C (10 min); 40 cycles at 95°C (15 s), 61°C (25 s), and 72°C (16 s). Specificity of the amplified product was confirmed by melting curve analysis. For relative quantification, a standard curve was generated from a six-step cDNA dilution series. Samples were amplified with primers for mL-FABP and 28 s rRNA. The relative expression of mL-FABP and 28 s rRNA were calculated from the standard curve. Relative quantity was calculated by the ratio of mL-FABP and the appropriate 28 s rRNA expression. The primer sequences in the real time reverse transcriptase-polymerase chain reaction were for mL-FABP 5′-CATCAAAAGAGCCTGGGAAC-3′ (forward), 5′-ACACCCATACG CCAACTCTT-3′ (reverse) and 28 s rRNA 5′-AACGGCGGGAG TAACTATGA-3′ (forward), 5′-TAGGGACAGTGGGAATCTCG-3′ (reverse).

Immunoblotting

Kidney tissue was homogenized in lysis buffer (50 mM Tris (pH 7.4), 100 mM NaCl, 2.5 mM ethylenediaminetetraacetic acid, 1% Triton X-100, 0.5% NP-40, 2.5 mM Na_3VO_4, 1 mM phenylmethylsulfonyl fluoride, 25 μg/ml aprotinin and leupeptin, and 50 μg/ml Soybean trypsin inhibitor) and sonicated briefly for 10 s subsequently centrifuged at 11 000 *g* for 10 min at 4°C, and the supernatant was collected. Protein concentration was measured using the protein assay kit (Bio-Rad Laboratories). Supernatants containing 50 μg of protein were separated on a 12% sodium dodecylsulfate-polyacrylamide gel electrophoresis and then electroblotted to a nitrocellulose membrane. The membrane was blocked for 1 h with 5% nonfat dried milk in TBS-T buffer (20 mM Tris, pH 7.6, 100 mM NaCl, 0.1% Tween 20). The primary antibodies used in our studies included polyclonal L-FABP antibody (Hycult Biotechnology, Uden, The Netherlands); rabbit anti-PMP70 antibody (Affinity Bioreagents, Golden, CO, USA), and rabbit polyclonal catalase antibody (Calbiochem, San Diego, CA, USA). These antibodies were used at a 1:1000 dilution and membranes were incubated overnight in TBS-T buffer containing 5% nonfat dried milk at room temperature. After washing three times with TBS-T buffer, the membranes were incubated with a horseradish peroxidase-conjugated goat anti-rabbit IgG as a second antibody (1:5000 dilution) for 1 h at room temperature. Proteins were visualized using by enzyme-linked enhanced chemiluminescence (Amersham, Arlington Heights, IL, USA). The membranes were stripped and then probed with β-actin antibodies (Chemicon, Temecula, CA, USA) as an internal control. Signals on the blots were visualized by autoradiography and quantitated by densitometry using ImageQuant image analysis system (Storm Optical Scanner; Molecular Dynamics, Sunnyvale, CA, USA).

Tissue preparation for immunohistochemistry

Kidney tissue samples were obtained from control-, WY-, CP-, and WY + CP-treated sv129 mice, and control-, CP-, Bz-, and Bz + CP-treated h-L-FABP transgenic mice. Tissues were fixed in 10% neutral-buffered formalin and embedded in paraffin. Sections (6 μm) were placed on silane-coated slides (Sigma, St Louis, MO, USA) and processed for morphologic analysis immunohistochemical localization of PMP-70, L-FABP, and for immunofluorescent staining of peroxisomes.

Morphologic analysis

Kidney sections were stained with PAS and the degree of morphologic damage was determined using light microscopy. The following parameters were graded to assess morphological damage after CP and Bz + CP treatment: brush border loss, red blood cell extravasation, tubular dilatation, tubular degeneration, tubular necrosis, tubular cast formation, interstitial edema, and inflammation. These parameters were evaluated on a scale of 0–4, which ranged from not present (0), mild (1), moderate (2), severe (3), and to very severe (4). Each parameter was determined at least on eight different animals. Statistical significance was assessed by the two-sided Student's *t*-test for independent samples.

PMP70 and L-FABP immunohistochemistry

To further ascertain that CP or fibrate affect the expression of PMP70, we performed immunostaining of mouse kidney tissue treated with CP or fibrate using a rabbit anti-PMP70 antibody (1:500 dilution; Affinity Bioreagents). In addition, since our Western blot analysis suggested that fibrate increased the expression of

L-FABP protein, we also performed immunostaining of mouse kidney tissue using a L-FABP polyclonal antibody that recognized mL-FABP (1:100 dilution; Hycult Biotechnology, Uden, The Netherlands), after which goat biotinylated anti-rabbit antibody (Vector Laboratories Inc., Burlingame, CA, USA) and ABC Elite Vectastain Kit (Vector Laboratories Inc.) was used. Nonspecific staining was blocked with 5% normal goat serum (Sigma), and the sections were permeabilized with 0.1% Triton X-100 (Sigma) and 0.05% saponin (Sigma) digestion. Endogenous peroxidase was inactivated with 1% hydrogen peroxide in phosphate-buffered saline/methanol (1:1).

Immunofluorescent staining of peroxisomes

To examine the effect of fibrate and CP on peroxisome proliferation in kidney tissue, we used a novel method of immunofluorescent labeling of peroxisomes, using an antibody to the PMP70, coupled with fluorescent nanocrystals, Quantum Dots.[24] This method is applicable to standard formalin-fixed and paraffin-embedded tissues. Paraffin sections were deparaffinized and hydrated in graded alcohol series and distilled water. Endogenous biotin sites were blocked by avidin/biotin blocking Kit (Vector Laboratories Inc.) according to the manufacturer's instructions. Nonspecific staining was blocked with 10% normal goat serum. The sections were incubated with rabbit anti-PMP70 antibody (diluted 1:500 in 10% normal goat serum; Affinity Bioreagents) for 1 h, then washed in phosphate-buffered saline and incubated for 30 min with (1:1000 dilution in phosphate-buffered saline) biotinylated goat anti-rabbit IgG (Sigma). After washing three times in phosphate-buffered saline, they were incubated with (1:100 dilution) 605 nm streptavidin-coated Quantum Dots (Quantum Dot Corp., Hayward, CA, USA). The sections were coverslipped and counterstained using mounting media containing 4,6-diamidino-2-phenylindole (Vector Laboratories Inc.). Fields for microscopic evaluation and subsequent image analysis were selected randomly. Fluorescent images were captured on a Zeiss LSM410 confocal microscope using a plan-apochromat $\times 63$ oil immersion objective with 1.4 numerical apertures. Blue, green, and red images were captured separately and overlaid. 4,6-Diamidino-2-phenylindole and quantum dot 605 fluorophores were excited with a 405 diode laser. Red-orange emitted light was detected after filtering with a 590–610 nm band pass filter, 4,6-diamidino-2-phenylindole-emitted light was filtered with a 435–485 nm band pass filter (D460/50m; Chroma Technology Corporation., Rockingham, VT, USA), and green auto-fluorescence was filtered through a 500–550 nm band pass filter (HQ525/50m; Chroma). The pixel density of the quantum dot signals were analyzed by Image J Software. Eight microscopic fields corresponding to the cortex area on pairs of adjacent sections (four microscopic fields/sections) from each animal kidney were chosen for area imaging in each treatment group. We quantified the pixel intensity of only orange/red color of quantum dot signals.

Measurement of urinary h-L-FABP protein

The enzyme-linked immunosorbent assay method for measuring urinary h-L-FABP was reported previously.[25,43,44] H-L-FABP protein standard or 50 μl of urine samples obtained from h-L-FABP transgenic mice are first treated with a pretreatment solution, and then transferred into a 96-well plate coated with a monoclonal antibody against h-L-FABP. After 1 h incubation, the wells are washed and then the conjugate reagent is added as secondary antibody for another hour allowing the binding of the h-L-FABP antigen, the immobilized antibody and the conjugate antibody. After incubation, the plate is washed and a substrate solution for the immunoperoxidase reaction is added for 30 min to develop a color based on the amount of h-L-FABP antigen present in the samples. h-L-FABP concentration is measured by measuring the absorbance of each well at 492 nm and calculated mass is determined based on a calibration curve. Urinary h-L-FABP levels is expressed as the ratio of the urinary h-L-FABP in micrograms to the urinary creatinine level (mg).

ACKNOWLEDGMENTS

This work was supported by National Institutes of Health Grant PO-1 DK 58324-01A5 and a VA Merit Award to Dr Didier Portilla. We acknowledge Dr Renu Bhatt for her technical help with the peroxisomal staining using quantum dots technique. A part of this study was supported by grants from the Health and Labour Science Research Grants for Research on Human Genome, Tissue Engineering, and Food Biotechnology from the Ministry of Health, Labour and Welfare of Japan (KN, EN, TS) and MEXT Leading Project (03023168) in Japan (EN).

REFERENCES

1. Chmurzynska A. The multigene family of fatty acid-binding proteins (FABPs): function, structure and polymorphism. *J Appl Genet* 2006; **47**: 39–48.
2. Zimmerman AW, Veerkamp JH. New insights into the structure and function of fatty acid-binding proteins. *Cell Mol Life Sci* 2002; **59**: 1096–1116.
3. Haunerland NH, Spener F. Fatty acid binding proteins – insights from genetic manipulations. *Prog Lipid Res* 2004; **43**: 328–349.
4. Huang H, Starodub O, McIntosh A *et al.* Liver fatty acid-binding protein colocalizes with peroxisome proliferator activated receptor-α and enhances ligand distribution to nuclei of living cells. *Biochemistry* 2004; **43**: 2484–2500.
5. Antonenkov VD, Sormunen RT, Ohlmeier S *et al.* Localization of a portion of the liver isoform of fatty acid-binding protein (L-FABP) to peroxisomes. *Biochem J* 2006; **394**: 475–484.
6. Reddy JK. Peroxisome proliferators and peroxisome proliferators-activated receptor-α. *Am J Pathol* 2004; **164**: 2305–2321.
7. Kaikaus RM, Chan WK, Ortiz de Montellano PR *et al.* Mechanisms of regulation of liver fatty acid-binding protein. *Mol Cell Biochem* 1993; **123**: 93–100.
8. Simon TC, Roth KA, Gordon JI. Use of transgenic mice to map cis-acting elements in the liver fatty acid-binding protein gene (Fabpl) that regulate its cell lineage-specific, differentiation-dependent, and spatial patterns of expression in the gut epithelium and in the liver acinus. *J Biol Chem* 1993; **268**: 18345–18358.
9. Oyama Y, Takeda T, Hama H *et al.* Evidence for megalin-mediated proximal tubular uptake of L-FABP, a carrier of potentially nephrotoxic molecules. *Lab Invest* 2005; **85**: 522–531.
10. Maatman RGHJ, Van de Westerlo EMA, Van Kuppevelt THMSM *et al.* Molecular identification of the liver- and the heart-type fatty acid-biding proteins in human and rat kidney. *Biochem J* 1992; **288**: 285–290.
11. Maatman RGHJ, Van Kuppevelt THMSM, Veerkamp JH. Two types of fatty acid-binding protein in human kidney. Isolation, characterization and localization. *Biochem J* 1991; **273**: 759–766.
12. Kamijo A, Sugaya T, Hikawa A *et al.* Urinary excretion of fatty acid-binding protein reflects stress overload on the proximal tubules. *Am J Pathol* 2004; **165**: 1243–1255.
13. Sugaya T, Noiri E, Yamamoto T *et al.* L-Type fatty acid-binding protein ameliorates renal ischemia reperfusion injury in human L-FABP transgenic mice. *Nephrology* 2005; **10**(Suppl): A133.
14. Portilla D, Dai G, Peters JM *et al.* Etomoxir-induced PPARalpha modulated enzymes protect during acute renal failure. *Am J Physiol Renal Physiol* 2000; **278**: F667–F675.
15. Portilla D, Dai G, McClure T *et al.* Alterations of PPARalpha and its coactivator PGC-1 in CP-induced acute renal failure. *Kidney Int* 2002; **62**: 1208–1218.
16. Portilla D. Energy metabolism and cytotoxicity. *Semin Nephrol* 2003; **23**: 432–438.
17. Li S, Wu P, Yarlagadda P *et al.* PPARalpha ligand protects during CP-induced acute renal failure by preventing inhibition of renal FAO and PDC activity. *Am J Physiol Renal Physiol* 2004; **286**: F572–F580.